Pathogenesis and autoimmunity initiated by a viral protein-induced apoptotic bodies

Heidi Pirttinen
Master's Thesis
University of Jyväskylä
Department of Biological and Environmental Science
Cell and Molecular Biology
8.1.2016

PREFACE

This thesis was conducted in the Cell and Molecular Biology Division in the Department of Biological and Environmental Science at the University of Jyväskylä. First and foremost, I want to express my gratitude to Dr. Leona Gilbert for giving me the opportunity to work in her research group. It has been an enjoyable and instructive journey. Secondly, enormous thanks to MSc. Kanoktip Puttaraksa: you have always been there for me, smiling and sharing your experience and knowledge and not ever have you lost your patience with me.

Huge thanks go to the whole Lee's research group, each and every one of you have supported and cheered me up through this project. The awesome environment you people created was something priceless!

From the bottom of my heart, I'd like to thank my awesome husband, my loving parents and family and all my wonderful friends for understanding me and encouraging me through my struggles with science. You always believed in me, even when my belief was lost.

Lastly, I would like to thank the funders of this project, Betty Väänänen Fund and Maaseudun Kukkasrahasto Säätiö for their precious financial support.

Laukaa 8.1.2016

Heidi Pirttinen

Jyväskylän yliopisto **Pro gradu – tutkielman tiivistelmä**
Matemaattis-luonnontieteellinen tiedekunta

Tekijä: Heidi Pirttinen
Tutkielman nimi: Virusproteiinin indusoimien apoptoottisten kappaleiden aiheuttama autoimmuniteetti
English title: Pathogenesis and autoimmunity initiated by a viral protein-induced apoptotic bodies
Päivämäärä: 8.1.2016 **Sivumäärä: 39**

Laitos: Bio- ja ympäristötieteiden laitos
Oppiaine: Solubiologia
Tutkielman ohjaaja(t): Leona Gilbert (FT, Dosentti), Kanoktip Puttaraksa (FM, jatko-opiskelija)

Tiivistelmä:

Ihmisen parvovirus B19 (B19) on laajalle levinnyt, yleinen virus, joka aiheuttaa lapsissa parvorokkoa (viides tauti). Aikuisille B19 aiheuttaa erinäisiä sairauksia, muun muassa nivelkipuja ja – tulehdusta, anemiaa, sekä raskaana oleville sikiöpöhöä. Lisäksi B19 infektio saattaa johtaa autoimmuunisairauksiin, kuten punahukkaan (*systemic lupus erythematosus*, SLE), nivelreumaan ja sydänlihastulehdukseen. Toisaalta infektio voi olla myös täysin oireeton. Mekanismit, jotka johtavat B19 tartunnasta autoimmuunisairauteen, ovat vielä tuntemattomia. Kuitenkin tiedetään, että B19:n ei-rakenteellinen proteiini NS1 on soluille tuhoisa ja aiheuttaa niiden kuoleman (apoptoosin) muodostaen solunjäännösten kanssa apoptoottisia kappaleita (ApoBodit). Nämä ApoBodit sisältävät itseantigeenejä sekä viruksen NS1 proteiinia. Tässä työssä tutkittiin B19 NS1 ApoBodien aiheuttamaa immuunireaktiota *in vivo* käyttäen hiiriä malliorganismina. Hypoteesina oli, että NS1 ApoBodit aiheuttavat hiirissä SLE:n kaltaisen autoimmuunireaktion, mikä ilmenee autovasta-aineiden tuottona, immuunisolujen tunkeutumisena kudoksiin sekä kudosvauriona. Hiiriin injektoitiin ApoBodeja kolmessa eri konsentraatiossa: 25 µg, 50 µg ja 100 µg. Hiiristä otettiin verinäytteet viikon päästä alkuperäisestä immunisaatiosta, ja viikolla neljä, ennen tehosteinjektion antamista. Kahdeksannella viikolla hiiret lopetettiin ja veri kerättiin seerumin eristystä varten. Aivot, sydän, munuaiset, maksa ja perna irrotettiin kudospatologista tutkimusta varten. Morfologisia ja patologisia muutoksia tarkasteltiin parafiiniin pedatuista, hematoksyliinilla ja eosiinilla värjätyistä kudosnäytteistä kirkaskenttämikroskopian avulla. Vasta-aineita kaksijuosteiselle DNA:lle (anti-dsDNA vasta-aineet) tutkittiin kaupallisella *Crithidia luciliae* immunofluoresenssitestillä, sekä tässä tutkimuksessa kehitetyllä entsyymivälitteisellä immunosorbenttimenetelmällä. Anti-dsDNA vasta-aineita, jotka ovat SLE:n biomarkkereita, havaittiin ApoBodeilla immunisoiduissa hiirissä molemmilla käytetyillä menetelmillä. Munuaisista, maksasta ja sydämestä löytyi immuunisolukeräytymiä. Lisäksi kaikkien hiirten aivoissa havaittiin neuronien rappeutumista, sekä demyelinaatiota kahdella suurimmalla ApoBodikonsentraatiolla. Samoilla hiirillä havaittiin myös sydänlihassolujen epäjärjestyneisyyttä, sekä sydänlihassolujen rappeumaa, joka oli nähtävissä jo alimmalla ApoBodikonsentraatiolla immunisoiduissa hiirissä. 50 µg:lla immunisoitujen hiirten pernassa oli muodostunut reaktiokeskuksia. Lisäksi valkoisen ytimen osuus hiirten pernasta kasvoi huomattavasti ApoBodikonsentraation myötä. Nämä löydökset tukevat hypoteesia. B19 NS1 ApoBodit tarjoavat elimistölle itseantigeenejä, johon immuunipuolustus reagoi ja näin ollen autoimmuniteetti saa alkunsa. Tämä tutkimus tarjoaa mekanismin B19 osallisuudesta autoimmuunisairauksien kehittymisessä. Lisäksi tässä tutkimuksessa kehitetty hiirimalli sekä mekanismi ovat sovellettavissa muiden patogeenisten virusten, kuten sytomegaloviruksen ja Epstein-Barr -viruksen tutkimiseen.

Avainsanat: Ihmisen parvovirus B19, ApoBodit, parvorokko, punahukka, autoimmuniteetti, DNA-vasta-aineet

University of Jyväskylä **Abstract of Master´s Thesis**

Faculty of Mathematics and Science

Author: Heidi Pirttinen
Title of thesis: Pathogenesis and autoimmunity initiated by a viral protein-induced apoptotic bodies
Finnish title: Virusproteiinin indusoimien apoptoottisten kappaleiden aiheuttama autoimmuniteetti
Date: 8.1.2016 **Pages: 39**

Department: Department of Biological and Environmental Science
Chair: Cell Biology
Supervisor(s): Leona Gilbert (PhD, Docent), Kanoktip Puttaraksa (MSc, PhD student)

Abstract:

Human parvovirus B19 (B19) is a widespread virus that infects people of all ages. In children, it usually causes an erythema infectiosum, a rash illness called the Fifth disease. In adults, it can cause arthralgia, arthritis, different types of anemia, and hydrops fetalis in pregnant women. Furthermore, the infection can lead to severe autoimmune diseases such as systemic lupus erythematosus, rheumatoid arthritis, myocarditis, liver, and kidney diseases. However, the B19 infection can sometimes be asymptomatic. The exact mechanisms by which B19 contributes to autoimmune diseases are still not known. However, the non-structural protein 1 (NS1) of B19 is known as a cytotoxic protein that induces apoptosis in host cells, thus forming apoptotic bodies (ApoBods) that contain self-antigens along with viral NS1 protein. Mice were used as a model organism in this study to investigate the effects of the NS1 ApoBods *in vivo*. It was hypothesized that the ApoBods initiate an SLE-like autoimmune disease in mice which manifests itself as autoantibody production, immune cell infiltration into the tissues, and tissue damage. Mice were inoculated with 25 µg, 50 µg, and 100 µg of B19 NS1 induced ApoBods. Blood was collected from the mice at week one, and four, before booster injections were administrated. At week eight, the mice were euthanized, blood was collected and serum isolated. Brain, heart, kidneys, liver, and spleen were dissected from each mouse for histopathological analysis. Sections embedded in paraffin, and stained with hematoxylin and eosin were studied for morphological and pathological changes with bright-field microscopy. Presence of anti-double-stranded DNA antibodies was investigated with a commercial *Crithidia luciliae* immunofluorescence test, and with a newly developed enzyme-linked immunosorbent assay. Anti-double-stranded DNA antibodies, which are the signature biomarker of SLE, were detected with both methods in the mice inoculated with B19 NS1 ApoBods. Immune cell infiltrates were detected in the kidneys, heart, and liver of the mice. In addition, neuronal degeneration was detected in the brain of all the mice treated with B19 NS1 ApoBods, and suspected demyelination was seen in the brain of the mice treated with 50 µg, and 100 µg of B19 NS1 ApoBods. Myocardial disarray was observed in the hearts of these two groups. Furthermore, in the hearts of all mice treated with B19 NS1 ApoBods, myocardial degeneration was detected. In the spleen of mice treated with 50 µg of the ApoBods, germinal centers had formed. Moreover, the proportion of the white pulp in the spleen was significantly increased by the dosage of ApoBods. These findings supported the hypothesis. B19 NS1 ApoBods cause inflammation by providing self-antigens to which the immune system reacts, and autoimmunity is initiated. Hence, this study provided a mechanism of B19 involvement in the pathogenesis of autoimmune diseases. Furthermore, this mechanism and model are applicable to studies of other viruses, such as cytomegalovirus and Epstein-Barr.

Keywords: Human parvovirus B19, SLE, NS1 ApoBods, anti-dsDNA antibodies, autoimmunity

TABLE OF CONTENTS

1 Introduction 8

1.1 Human parvovirus B19 9

1.2 Clinical manifestations and relevance of B19 infection 9

1.3 SLE in humans and mice 10

2 Aims of the study 12

3 Materials and methods 12

3.1 Production and purification of ApoBods 13

3.2 Serum collection and analysis 14

3.2.1 *Crithidia luciliae* immunofluorescence test (CLIFT) 14

3.2.2 Anti-dsDNA ELISA 15

3.3 Histopathology 16

3.3.1 Sectioning 16

3.3.2 H&E Staining 17

3.3.3 Bright-field imaging and image processing 18

4 Results 18

4.1 Anti-dsDNA antibody production was initiated in the mice treated with B19 NS1 ApoBods 18

4.1.1 CLIFT 18

4.1.2 Anti-dsDNA ELISA 22

4.2 Inflammation and tissue damage were initiated by B19 NS1 ApoBods 24

5 Discussion 30

5.1 B19 NS1 ApoBods induced autoantibody production 30

5.2 B19 NS1 ApoBods initiated autoimmunity and SLE-like disease in mice 31

6 Conclusions 35

7 References 36

ABBREVIATIONS

Anti-dsDNA antibodies	Anti-double-stranded DNA antibodies
ApoBods	Apoptotic bodies
BALB/cOlaHsd	Laboratory mouse strain used in, for example, autoimmunity research
B19	Human parvovirus B19
CLIFT	*Crithidia luciliae* immunofluorescence test
ELISA	Enzyme-linked immunosorbent assay
NS1	Non-structural protein 1 of Human parvovirus B19
PBS	Phosphate-buffered saline
Pristane	2,6,10,14-tetramethylpentadecane
RT	Room temperature
SLE	Systemic lupus erythematosus

1 INTRODUCTION

Various human diseases are caused by viruses. Some of these viruses are transient and easily cleared by the immune system while others may cause chronic infections, lead to autoimmunity or cancer. Normally, the immune system protects the body from pathogens such as viruses (Baron, 1996). Upon infection, B lymphocytes produce antibodies that bind to the viral antigens, thus neutralizing them (humoral immunity). In addition, the body fights against viral infections by cell-mediated immunity. Leukocytes such as macrophages may recognize and kill the virus and the cells infected with it. Furthermore, they can activate other cells by secreting cytokines that message them to mature and proliferate. Usually, the infection is cleared, and a population of memory cells lingers in the body protecting from future infections of the same virus. If, however, the virus has not been cleared and it persists, immune complexes may build up and damage tissues. This will lead for example, to nephritis or vascular damage.

The break of self-tolerance is a serious complication of the immune system. It might happen due to abnormal apoptosis rate (either too much or too little) or defective clearance of apoptotic bodies (ApoBods) (for review see Elmore, 2007; Jung and Suh, 2015). Apoptosis, or programmed cell death, is a normal cellular event (Kerr et al., 1972). The cell shrinks, and the chromatin condenses into dense particles (nucleus becomes pyknotic) (for review see Elmore, 2007). The formation of ApoBods also occurs normally in spontaneous apoptosis and ApoBods are phagocytosed and degraded (Kerr et al., 1972). Cell organelles bud out of the plasma membrane with or without nuclear fragments. By phagocytosing these ApoBods (cellular leftovers), the system gets rid of extra cellular material, also removing self-antigens (for review see Elmore, 2007). However, if this system malfunctions, it may lead to autoimmunity. Jung and Suh (2015) stated that autoimmune disease systemic lupus erythematosus (SLE) originates from this particular reason. Incomplete disposal of ApoBods consequently results in B cell activation and autoantibody production. Thus, ApoBods break tolerance and initiate autoimmunity that becomes a self-sustaining loop with a continuous supply of self-antigens. In SLE, especially anti-double-stranded DNA (anti-dsDNA) antibodies are produced. They are autoantibodies against native DNA from the organism itself. SLE is discussed later in more

detail. Pathogens included in the ApoBods may additionally contribute to the initiation of autoimmunity. One interesting example of these is human parvovirus B19.

1.1 Human parvovirus B19

Human parvovirus B19 (B19) was discovered in 1974 (Heegaard and Brown, 2002). It is a DNA virus with a single-stranded genome (Clewley, 1984) that codes for two structural proteins, viral protein 1 and 2 (minor 84 kDa, and major 58 kDa capsid proteins, respectively) (Heegaard and Brown, 2002). Furthermore, it codes for several non-structural (NS) proteins, two of them (11 kDa and 7.5 kDa) with unknown functions and one being cytotoxic superfamily three helicase protein, known as NS1 (77 kDa) (Raab et al., 2002; Lehmann et al., 2003). B19 replicates only in erythroid progenitor cells (for review see Young and Brown, 2004). In non-permissive cells, such as liver cells (Poole et al., 2006), over expression of NS1 initiates apoptosis by damaging DNA (Poole et al., 2011). Moreover, ApoBods consisting of NS1 protein, nuclear, and cytosolic self-antigens, are formed *in vitro*.

B19 NS1 induced ApoBods contain apolipoprotein-H, DNA, histone H4 and lysosomal self-antigens, amongst others (Thammasri et al., 2013). Self-antigens are proteins derived from the host itself and in a fully functional immune system, they are ignored. However, B19 NS1 ApoBods are recognized and engulfed by macrophages in cell cultures. Moreover, these antigens mentioned above, are suggestive of an autoimmune condition. Hence, B19 NS1 ApoBods could initiate immune reaction to self.

1.2 Clinical manifestations and relevance of B19 infection

B19 is a common virus seen all over the world. Fifty to 70 % of adult population has IgG antibodies against B19 (Söderlund-Venermo et al., 2002). B19 infection usually causes a rash, erythema infectiosum (fifth disease) in children. In adults, it may cause arthritis, aplastic anemia, fetal hydrops in pregnant women, and other complications such as liver dysfunction. Occasionally, B19 causes fulminant liver failure or hepatitis in previously healthy individuals (Krygier et al., 2009; Hatakka et al., 2011). Various autoimmune diseases such as SLE, rheumatoid arthritis, and vasculitis are associated with B19 infection. Not surprisingly, B19 infection often coincides with autoantibody production (Hemauer et al., 1999). These antibodies include antiphospholipid, antinuclear antibodies,

rheumatoid factor, and antilymphocyte antibodies. In addition, B19 is also associated with myocarditis (Feldman and McNamara, 2000; Bültmann et al., 2003; Kühl et al., 2003). Kühl and others (2003) found viral DNA in heart tissue even though no infiltrates were detected. In contrast, Bültmann et al. (2003) reported a case of myocarditis clinically similar to ischemic heart disease with marked infiltrations. Interestingly, SLE has been mentioned as one of the common causative agents of myocarditis (Feldman and McNamara, 2000). This might suggest that B19 could be the instigator of myocarditis also with relation to SLE. The early and accurate diagnosis and treatment of this viral infection could help to prevent the onset of more severe and prolonged effects.

1.3 SLE in humans and mice

SLE is an inflammatory autoimmune disease with diverse clinical manifestations, and typically expressing anti-nuclear autoantibodies. In general, SLE involves multiple organs such as kidneys, brain, and heart (Mok and Lau, 2003) in genetically susceptible subjects and most often, affects females (Wahren-Herlenius and Dörner, 2013). Several studies imply that SLE is associated with faulty clearance of apoptotic debris (Shao and Cohen, 2011), thus leading to a continuous supply of self-antigens and inflammation. Especially neutrophils are related to the damage in organs targeted in SLE (Wahren-Herlenius and Dörner, 2013). Their presence correlates with disease activity, nephritis, and vasculitis.

Production of autoantibodies, poor regulation of pro- and anti-inflammatory cytokines, and overt activeness of immune cells all contribute to continuous organ inflammation in SLE (for review see Jung and Suh, 2015). The most important lupus-indicator of these is the presence of anti-dsDNA antibodies. They are a marker for SLE because they are solely found in SLE patients. Furthermore, they are strongly associated with glomerulonephritis although this relation is not absolute: one may exist without the other (Mok and Lau, 2003). Anti-dsDNA antibodies can be detected in patients even years before the actual disease manifests itself (Yung and Chan, 2007). When isolated either from human or mouse, these antibodies are capable of inducing a nephritis-like disease in mice, although they are not the only contributor in pathogenicity of lupus nephritis.

A variety of mouse models has been developed to investigate the pathogenesis of SLE. Some mouse strains develop SLE spontaneously and in some it can be induced, for example, by pristane. Furthermore, several genetically modified mouse models have been

developed to investigate certain genetic aspects in SLE pathogenesis. NZB/W, a first filial generation hybrid between New Zealand Black and New Zealand White mice, is a model with severe manifestations much alike to those in humans (for review see Perry et al., 2011). These mice develop lymphadenopathy, splenomegaly, antinuclear antibodies, and glomerulonephritis leading to death at 10-12 months of age. Lupus in NZB/W mice affects mostly females. In contrast, both sexes of MRL/lpr mice are affected. This strain develops SLE spontaneously, which is seen as lymphadenopathy, and high concentrations of autoantibodies (antinuclear, anti-DNA, anti-Sm, rheumatoid factor). A vast amount of immune complexes forms of these autoantibodies. Mortality of this mouse strain is faster than that of the other strains. Lupus in BXSB/Yaa mice is more severe and starts earlier in males than females. Males live about five months whereas females survive 14 months most commonly dying of proliferative glomerulonephritis. Other features of lupus are monocytosis, hypergammaglobulinemia, autoantibodies against nuclear and erythrocytic antigens, retroviral glycoprotein (gp70) titers, and secondary lymphoid tissue hyperplasia. All of these strains mentioned earlier have distinct benefits and indications that apply to different areas of SLE research, mainly the involvement of genetics.

Environmental contributors of SLE can be studied in induced mouse models such as that induced by intraperitoneal injection of 2, 6, 10, 14 tetramethylpentadecane (pristane) (for review see Perry et al., 2011). BALB/c mice are commonly used in this model, but almost all mouse strains are inducible (for example DBA/1 and SJL) (Bender et al., 2014). Pristane injection induces various lupus-associated autoantibodies in BALB/c mice at concentrations comparable to that in MRL/lpr mice. In addition, nephritis is initiated by immune-complex deposition and proteinuria in BALB/c mice. Furthermore, these mice present lung involvement and arthritis after pristane treatment.

Another inducible lupus model is induced graft-versus-host disease model where lupus is induced by lymphocytes from a host of a different generation (for review see Perry et al., 2011). This leads to immunological deficiencies, type of which is dependent on the model used. In addition, lupus mouse models, especially those that develop lupus spontaneously, are used for therapeutic studies. These studies target for example cytokines secreted by lymphocytes, receptors, and other factors in cell signaling pathways, and hormones. However, only one strain is not sufficient to validate the efficacy of a drug and even if many strains are used, the drug might be of use in only some patients. Nevertheless, lupus

mouse models have a strong foothold in lupus research and further amelioration of lives of the patients.

2 AIMS OF THE STUDY

B19 is hypothesized to be a contributor to SLE and other autoimmune diseases. The mechanism of its pathogenicity is not fully known, although NS1 has been shown to have a significant role. The purpose of this study was to investigate the autoimmune reaction caused by B19 NS1 induced ApoBods *in vivo* using mice as a model organism. Furthermore, tissue damage caused by processing of these ApoBods and immune cell infiltration into the tissues were the primary focus. Brain, heart, kidneys, liver, and spleen were investigated since they are the main target organs in SLE pathogenesis (Mok and Lau, 2003; for review see Gulinello and Putterman, 2010). Also, anti-dsDNA antibodies were of interest because their presence is an indicator of SLE. Hypothesis was that NS1 propagated ApoBods induce autoimmunity, thus, autoantibodies and especially anti-dsDNA antibodies can be detected in serum. Furthermore, immune cells infiltrate into the tissues and cause inflammation. Tissues are damaged because of the occurring immune reaction.

3 MATERIALS AND METHODS

Mice were used as a model organism to study the effects of B19 NS1 ApoBods *in vivo*. 27 inbred BALB/cOlaHsd female mice were acquired from Harlan®, Netherlands, with permission from ELLA, Animal Experiment Board in Finland (ESAVI 6098). Mice were randomly divided into nine treatment groups, three in each. One group was left untreated as a negative control, and another negative control group received phosphate-buffered saline (PBS), which was used as a diluent for the ApoBods. Three groups were inoculated with 25, 50, and 100 µg (/30 g mouse body weight) B19 NS1 ApoBods and three groups received the same concentrations of staurosporine-induced ApoBods. ApoBods concentrations were determined in previous studies by Western blots: 25 µg of ApoBods was the lowest concentration showing detectable autoantigens (unpublished data). Positive

control group was injected with 0.782 g/mL of 2,6,10,14-tetramethylpentadecane (pristane). Staurosporine ApoBods were a positive control for apoptotic induction and pristane was a control for autoimmunity (Reeves et al., 2009). Pristane induces autoantibody production and lupus in mice.

Blood was collected from the tail vein of the mice at week one, and four. After the blood collection at week four, the mice were given subcutaneous booster injections to obtain sufficient antibody titers in the blood. Pristane group received both injections intraperitoneally. At week eight, the mice were euthanized with a mixture of 1.0 mg/kg of Domitor and 75 mg/kg of Ketalar administrated by intraperitoneal injection.

3.1 Production and purification of ApoBods

ApoBods were produced according to the protocol described by Thammasri et al. (2013). Briefly, B19 NS1 ApoBods were produced with Bac-to-Bac® Baculovirus Expression system (Invitrogen, CA, USA) in which the recombinant viruses were expressing NS1. Spodoptera frugiperda –cells (Sf9) (ATCC-CRL-1711, Manassas, VA, USA) were grown in Insect-Xpress cell medium (BioWhittaker®, Walkersville, MD, USA) at 27 °C to harbor the virus. Human hepatocellular carcinoma cells (HepG2 cells, ATCC-HB-8065) were cultured in Minimum Essential Medium (Gibco®) supplemented with 10 % fetal bovine serum (Gibco®), 1 % penicillin-streptomycin (Gibco®), and 1 % L-glutamine (Gibco®) at +37 °C, 5 % CO_2 to determine the transduction efficiency of the third generation virus as described by Kivovich et al. (2010). To produce ApoBods, 10 x 10^6 of HepG2 cells were seeded in cell culture flasks and grown at 37 °C in 5 % CO_2 for 24 h and transduced with the recombinant viruses (transduction efficiency 50-70 %) by rocking them in the dark, at room temperature (RT) for 4 h. Cells were washed with sterile PBS, and warm medium added and incubated at 37 °C in 5 % CO_2 for 72 h.

At 72 h post-transduction, the supernatants were centrifuged (Heraeus Labofuge 400, Thermo Fisher Scientific Inc., UK) at 1 700 x g for 3 min and filtered through a 5.0 µm filter. Filtered supernatants were ultracentrifuged at 285 000 x g (Beckman Coulter Optima L-90K Ultracentrifuge) for 1 h at 4 °C. Pellets were resuspended in 100 µL PBS overnight at 4 °C. Staurosporine ApoBods were produced similarly except that they were not transformed with baculoviruses but with 1 µM staurosporine in the growth medium.

3.2 Serum collection and analysis

Blood was collected from the mice at week one, four and eight. At week one and four, blood was collected from the tail vein. After injection of Domitor/Ketalar mixture at week eight, blood was drawn by cardiac puncture. The blood from each mouse was put into an eppendorf tube and left to clot at room temperature (RT) for 45 min. Tubes were centrifuged (Thermo Scientific) at 2000 rpm for 20 min at RT. Serum (upper layer) was pipetted into a new tube, and the blood tube was left again for 30 min at RT, and then re-centrifuged at 2000 rpm for 10 min at RT. Serum was collected again in the same serum tube and stored at -20 °C.

3.2.1 *Crithidia luciliae* immunofluorescence test (CLIFT)

Anti-dsDNA antibodies were tested from the sera from week eight by commercial CLIFT test (IIFT *Crithidia luciliae* sensitive (anti-dsDNA), Euroimmun AG, Germany). The kit contained all reagents needed for the test, except fluorescein-labelled anti-mouse secondary antibody (Euroimmun AG, Germany) was ordered separately. Sera samples were diluted 1:10 with sample buffer 2 and 30 µL of each dilution was pipetted to a reagent tray supplied in the kit. BIOCHIP slides (slides with 10 BIOCHIPS containing *Crithidia luciliae* –cells) were placed upside down on top of the reagent tray so that each chip came into contact with its corresponding sample. Autoantibody against dsDNA from human serum (provided in the kit) was used as a positive control and diluted to 1:32 with PBS-Tween (0.2 % Tween20 in PBS). As a negative control for the kit, autoantibody negative human serum was used, also in 1:32 dilution. The kit is developed for human diagnostics, thus the human controls were used. Furthermore, the negative sera (untreated and PBS-treated) would act as negative controls of the test. After adding the sera samples, the slides were incubated for 1 h, at RT. Then they were dipped quickly in PBS-Tween and immersed in a 50 mL Falcon tube containing 35 mL PBS-Tween. Slides were washed for 10 min with a rotary shaker.

Fluorescein-labelled goat anti-human secondary antibody (Euroimmun, Germany) was used with positive and negative control. Goat anti-mouse secondary antibody (IgG) (Euroimmun, Germany), also labelled with fluorescein, was used for mouse sera samples. Secondary antibodies were protected from light, and they both were diluted 1:10 with sample buffer 2. 25 µL of that dilution was pipetted to the recesses on the reagent tray. One

slide at a time was removed from PBS-Tween, back and long sides of the slide dried with a paper towel and the slide immediately put onto the reagent tray so that each BIOCHIP was in contact with its sample. Slides were incubated for 30 min, in the dark, at RT.

Slides were rinsed as described above and shaken for at least 5 min on a rotary shaker. Embedding medium (glycerol, provided) was placed on the coverslip, every side except between the BIOCHIPs of the slide was dried with a paper towel and the slide angled upside down onto the coverslip. Slides were let dry at RT, protected from light and then moved to +4 °C for storage. Slides were protected from light at all times since addition of secondary antibody.

Fluorescent patterns were detected with Leica DM5500 fluorescence microscope with a 40x (Leica HCX PL Fluotar, numerical aperture 0.75) objective. Furthermore, differential interference contrast images were acquired simultaneously with fluorescence images with a Leica DFC310 Fx camera to confirm that all cells were fluorescent. Images were processed with an open source software ImageJ (Rasband, NIH, USA), sharpened and brightness and contrast of differential interference contrast images were adjusted when needed. At least six images per sample were taken, always in the same order. From each mouse, 300 cells in total were counted from the images. Positively stained (kinetoplast stained near flagella) *Crithidia* cells were counted out of the 300.

3.2.2 Anti-dsDNA ELISA

Mouse sera collected at three different time points was tested with an ELISA method developed from a protocol used in human diagnostics of B19 (unpublished data). 96-well microplates (Nunc MicroWell, Thermo Scientific Inc. Finland) were coated with mouse double-stranded DNA isolated from healthy mouse tissues (Dneasy Blood and Tissue kit, Qiagen, Germany). DNA was diluted to 0.01 µg/µL with 0.1 M carbonate buffer (0.1 M Na_2CO_3 + 0.1 M $NaHCO_3$, pH 9.5). Wells were coated with 1 µg/µL DNA in carbonate buffer. For background measurement (blank), three wells/plate were left uncoated. As a positive control for the assay, normal mouse IgG (3 mg/mL) (Molecular Probes, Life Technologies) was used in 1:5 000 dilution in carbonate buffer. Plates were covered with lids and incubated at +4 °C, overnight. All solutions, including DNA dilutions as well as the plates, were stabilized to RT before use.

At day two, plates were washed three times and blocked. Firstly, wells were emptied by inverting the plates, dried by gently pressing upside down on a paper towel and filled with 300 µL washing solution (0.05 % Tween20 in PBS, pH 7.4). Wells were soaked for 5 min, emptied as described and washed twice with 300 µL/well of washing solution. Microplate washer (Nanjing Perlove Medical Equipment) was used in washing except for soaking steps. After emptying the plates, 200 µL of the blocking solution, 2 % bovine serum albumin dissolved in phosphate-buffered saline (BSA/PBS), was added per well and incubated at + 4 °C, overnight.

After blocking, plates were washed five times as described above. Sera samples were diluted 1:200 with 1 % BSA/PBS and 100 µL of dilutions were added to the wells. All sera were tested in triplicates. For blank and positive control, 100 µL of 1 % BSA/PBS was added. Plates were incubated 2 h, at RT and then washed five times as previously described. Horseradish peroxidase conjugated goat anti-mouse IgG secondary antibody (Novex, Life Technologies) was diluted 1:1000 in 1 % BSA/PBS, 100 µL added to the wells and incubated 1.5 h, at RT. Plates were washed again five times as described and 100 µL 3,3',5,5'-tetramethylbenzidine (TMB) –substrate (Thermo Scientific) was added and incubated 30 min, at RT in the dark (covered with foil). 100 µL of 2 M sulphuric acid stop solution was added, plates tapped gently to mix the solutions, and absorbance measured (Perkin Elmer Victor X4) at 450 nm for 0.1 s.

The cut-off value was calculated from three standard deviations plus the mean of all negative control sera (untreated and PBS groups). Because two plates were used for testing of each time point, mean of both blank values was used as a blank for calculations. It was subtracted from absorbance values of every triplicate. The mean absorbance - blank from all three mice per group were calculated.

3.3 Histopathology

3.3.1 Sectioning

Brain, heart, kidneys, liver, and spleen are the target organs in SLE (Mok and Lau, 2003; for review see Gulinello and Putterman, 2010). Organs were dissected according to standard operation procedures (Ruehl-Fehlert et al., 2003) and trimmed to remove fat as well as other extra tissue. Trimmed organs were cut into 3-5 mm pieces. Parts of the organs

described by Ruehl-Fehlert et al. (2003) were fixed in 10 % formalin at RT for 48 h. After fixing, the tissues were transferred into 70 % ethanol for 48 h. Tissues were kept immersed in 70 % ethanol and placed in metal embedding baskets. Automated tissue processor (Shandon Duplex) was used to embed the samples in paraffin. Tissues were dehydrated by gradually increasing the concentration of ethanol: twice with 70 %, once 80 % and 95 % ethanol, 1 h in each and finally three times with 100 % ethanol, 1.5 h each. Ethanol was removed from the tissues with three changes of xylene (Sigma-Aldrich), each for 1.5 h. Tissue baskets were dipped in paraffin wax heated to 58 °C in two separate containers for 2 h each. Tissues were placed in plastic embedding cassettes so that the cut surface was facing towards the surface of the upcoming block. Paraffin was added from a dispenser and blocks were let to harden. In the interest of saving time, Riitta Vuento, University of Oulu, kindly sectioned the blocks, and I, however, sectioned one sample of every organ. 5 µm sections were cut with a sliding microtome (Leica) and then put into 40 °C water bath. Two slices of each sample were picked onto an objective glass. Glasses were dried for at least 30 min at RT and then stored at RT for staining.

3.3.2 H&E Staining

Paraffin was melted from the mounted sections by incubating on a 58 °C heat block for 15 min. Sections were cleared in three changes of xylene, 5 min in each and hydrated with descending concentrations of ethanol: two changes of 100 % ethanol, one 95 %, 80 % and 50 % ethanol, 3 min each. Thereupon the objective glasses were rinsed in distilled water for 5 min and stained.

Staining was conducted in glass basins. Objective glasses were first immersed for 5 min in Accustain Harris Hematoxylin (Sigma-Aldrich), rinsed in distilled water for 30 s and under slowly running tap water for 5 min to develop stain. For de-staining, objective glasses were dipped 20 times in 10 seconds in acid-ethanol (0.25 % HCl in 70 % ethanol). Glasses were rinsed under slowly running tap water and in distilled water, both for 2 min. Excess water was shaken off and the glasses dried by touching a paper towel before staining them 40 s with eosin (Sigma-Aldrich). Three changes of 95 % and 100 % ethanol, 5 min each, and three changes of xylene, 15 min per change, was used to dehydrate the samples. Coverslips were mounted with DPX Mountant for Histology (Sigma Life Science) and the slides stored at +4 °C.

3.3.3 Bright-field imaging and image processing

Tissues were examined using bright-field imaging (Leica DM5500). At least ten images per each sample were acquired with Leica DFC310 Fx color camera, with the same brightness and contrast settings. All tissue samples were investigated with a 20X (Leica HCX FL PLAN, numerical aperture 0.40) and a 40X (Leica HCX PL Fluotar, numerical aperture 0.75) objectives. However, images were acquired from brain, heart, liver, and spleen with 20X magnification and with 40X from the kidneys. Images were processed with an open-source software ImageJ (Rasband, NIH, USA) for scale bar additions. Sharpness, brightness and contrast were adjusted, and final panel figures were created with a licensed software Adobe Photoshop Elements 11 (Adobe Systems Inc. USA).

4 RESULTS

4.1 Anti-dsDNA antibody production was initiated in the mice treated with B19 NS1 ApoBods

Sera samples were stored at -20 °C and thawed on ice when needed. After thawing, samples were aliquoted. The presence of anti-dsDNA antibodies was studied with two different techniques. Commercial CLIFT-test (Euroimmun AG, Germany) was used only for the sera samples from the week eight serum collection. However, sera from every time point, week 1, 4, and 8, were tested with the newly developed ELISA method.

4.1.1 CLIFT

In negatively stained samples, generally the base of flagella alone was stained as seen in Figure 1a (untreated) and 1b (PBS-treated) as a single green spot in one cell. A negatively stained *Crithidia* cell is pointed out in Figure 1b with letters “nc”. The staining pattern is positive when the kinetoplast next to flagellum is stained. Figure 1 illustrates representative staining patterns from each treatment group. Close-up images in lower left corners of panels in Figure 1 are zoomed images of representative staining pattern in each panel. Negative staining pattern in the CLIFT assay is illustrated in Figure 1a and 1b (untreated and PBS-treated, respectively). The positive staining pattern is represented in Figure 1c acquired from the pristane-treated mice. A positively stained *Crithidia* cell is

pointed out by the letters “pc”. The positive staining indicates the presence of anti-dsDNA antibodies, which in turn refers to SLE. The *Crithidia* cells stained positively when incubated with sera from pristane-treated (Figure 1c), 25 µg (Figure 1d), 50 µg (Figure 1e), and 100 µg (Figure 1f) B19 NS1 ApoBods, 25 µg (Figure 1g), 50 µg (Figure 1h), and 100 µg (Figure 1i) staurosporine ApoBods treated mice. However, few positive cells were observed as well in untreated (1a) and PBS (1b). The intensity of fluorescence of the negative sera (untreated and PBS, Figure 1a and 1b, respectively), was not as strong as it was in the sera from mice treated with pristane (Figure 1c) or either ApoBods (B19 NS1 ApoBods Figure 1d-f, and staurosporine ApoBods Figure 1g-i). Negative control of the kit was completely negative (no staining of kinetoplast), and the positive control was positive (data not shown). The control images were left out since they illustrate only the staining patterns which can also be seen from the test images.

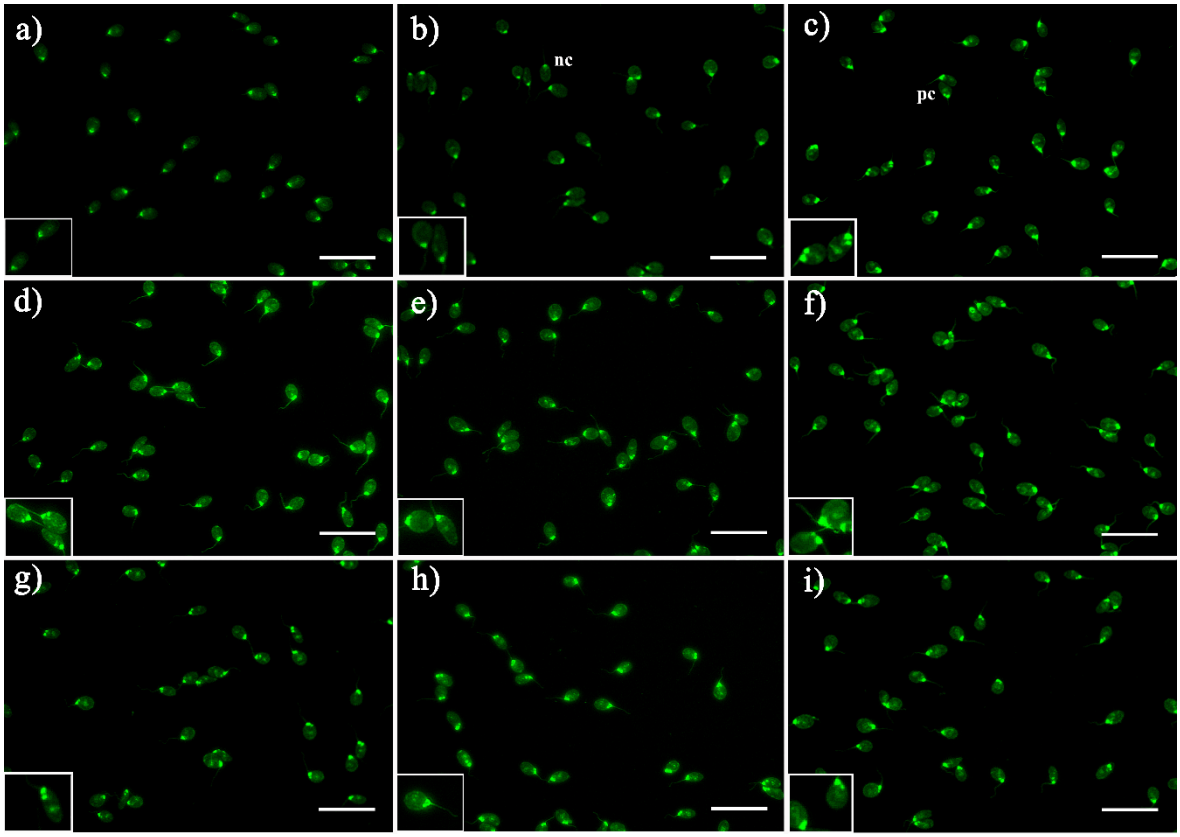

Figure 1. CLIFT test for anti-dsDNA antibodies from mice serum. Representative fluorescence images of treatment groups: a) untreated, b) PBS, c) pristane, d) 25 µg, e) 50 µg, and f) 100 µg B19 NS1 ApoBods, g) 25 µg, h) 50 µg, and i) 100 µg staurosporine ApoBods. Original magnification 40x, scale bar = 200 µm. nc = negatively stained cell, pc = positively stained cell. Close-ups are zoomed images from each panel. Cells stained positively with sera from every group in varying extent.

Three hundred cells were counted from the images of each serum sample. Out of these 300 cells, the positive cells were manually calculated based on visually observed staining patterns. Positive *Crithidia* cell staining is illustrated in Table 1. Positive cell count and percentage are presented for each mouse (numbered from one to 27), and treatment groups are indicated on the rows highlighted in green. Only two mice of six negative controls (untreated and PBS, three mice in each) were truly negative (mouse 1 and 5; in both 1.3 % positive). A great variation between the mice in each group is evident. Every mouse is an individual that can react differently to the treatments. 1:10 dilution of the sera were used as advised by the kit, thus the threshold for a positive result was kinetoplast fluorescence at dilution 1:10. In this case, however, the threshold should be determined as a value out of 300 cells. In automated CLIFT readings, the intensity of the fluorescence is measured, and the threshold is determined by intensities of fluorescence (Gerlach et al., 2015). Based on these cell counts, the average positive percentage in each treatment group was calculated and is depicted in Figure 2. Treatment groups are depicted as the function of the mean percentage of positive cells. Based on these results, it is difficult to contrast the effect of the different treatments. The number of positive cells seems not to correlate with the dose either. In every group except PBS-treated and 50 µg B19 NS1 ApoBods at least half of the cells were positive.

Table 1. *Crithidia luciliae* immunofluorescence test results. Positive cells out of 300 were counted. The percentage of positives was calculated from 300 cells. Cell counts are illustrated per each mouse in each treatment group.

Treatment	Untreated			PBS			Pristane		
Mouse number	1	2	3	4	5	6	7	8	9
Positive cells/300	4	258	241	200	4	32	263	152	169
Positive [%]	1.3	86.0	80.3	66.7	1.3	10.7	87.7	50.7	56.3

Treatment	25 µg B19 NS1 ApoBods			50 µg B19 NS1 ApoBods			100 µg B19 NS1 ApoBods		
Mouse number	10	11	12	13	14	15	16	17	18
Positive cells/300	147	227	206	130	89	89	124	206	175
Positive [%]	49.0	75.7	68.7	43.3	29.7	29.7	41.3	68.7	58.3

Treatment	25 µg Staurosporine ApoBods			50 µg Staurosporine ApoBods			100 µg Staurosporine ApoBods		
Mouse number	19	20	21	22	23	24	25	26	27
Positive cells/300	48	206	219	219	168	234	187	54	229
Positive [%]	16.0	68.7	73.0	73.0	56.0	78.0	62.3	18.0	76.3

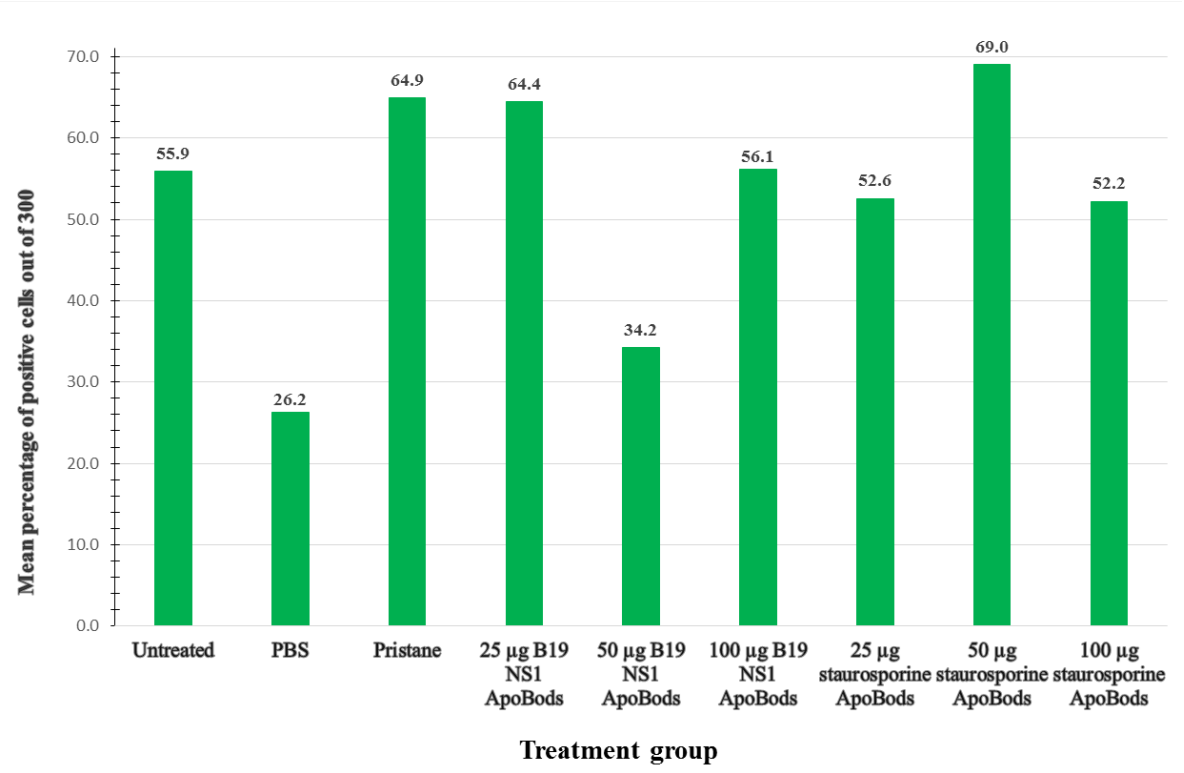

Figure 2. CLIFT test results by treatment groups from serum collection at week eight. 300 *Crithidia* cells in total were counted, out of which the percentages of positive cells (kinetoplast stained) were determined. Mean of the positive cells (percentages out of 300) in each group is presented. Positive staining of the cells indicates the presence of dsDNA in the serum.

Anti-dsDNA antibodies were tested with CLIFT first from the serum collection from week eight because that time point was most likely to show antibodies. However, negative sera (untreated and PBS) should not present anti-dsDNA antibodies and they should not stain positively. Thus, sera from time points of week one and four were tested only with ELISA method whereas the sera from week eight were tested with both methods. The fact that each mouse has its individual immune system that might react differently to the same treatment in two mice might have caused the variation inside each treatment group.

4.1.2 Anti-dsDNA ELISA

Anti-dsDNA antibodies were detected from the serum collected from three time points (week one, four, and eight) with ELISA method. The absorbance of the samples was measured at 450 nm for 0.1 s. Mean of blank absorbance values was deducted from the mean absorbance values of all the negative sera samples (untreated and PBS). Three standard deviations of all negative samples were added, thus obtaining the cut-off values of 0.574, 0.760, and 0.591 for week one, four, and eight, respectively. The mean of the blanks

was deducted from all absorbance values, and mean absorbance values of each treatment group from every serum collection are presented in Figure 3. Absorbance values above the cut-offs of each week (0.574, 0.760, and 0.591 for week 1, 4, and 8, respectively) are positive. Accordingly, after week one, mice treated with 50 µg and 100 µg B19 NS1 ApoBods were positive (0.650 and 0.838, respectively). Furthermore, only pristane group was positive (0.810) at week four and week eight, 50 µg and 100 µg B19 NS1 ApoBods and pristane group were positive (0.736, 0.774, and 1.150 respectively) for anti-dsDNA antibodies.

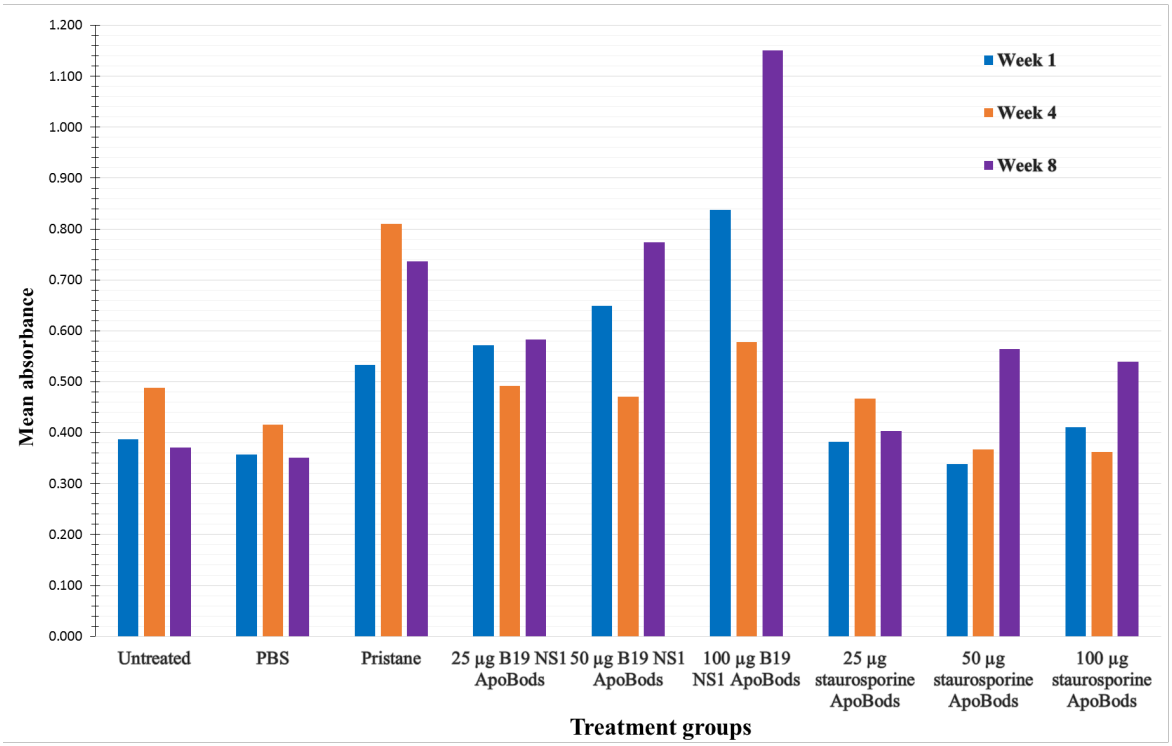

Figure 3. Anti-dsDNA ELISA. Absorbance values were measured at 450 nm for 0.1 s. Blank values were subtracted and mean of each treatment group was calculated. Mean values per treatment group are shown of all three serum collection time points. Blue bars represent week one serum collection, orange week four, and purple week eight. Cut-off values were 0.574, 0.760, and 0.591, respectively, with three standard deviations. After week one, 50 µg and 100 µg B19 NS1 ApoBods treated mice were positive (0.650 and 0.838), after week four only pristane (0.810), and after eight weeks pristane and the groups mentioned above were positive (0.736, 0.774, and 1.150, respectively) for anti-dsDNA antibodies.

4.2 Inflammation and tissue damage were initiated by B19 NS1 ApoBods

H&E stained sections of every organ were examined with bright-field microscopy. The morphology, possible damage, and all other abnormalities were screened. Cerebral cortex and hippocampus were examined from the brain. Normal brain architecture is illustrated in Figure 4a and 4b by untreated and PBS treatment groups, respectively. Cells were distributed evenly in the tissue, either degenerative changes or demyelination was not observed. However, degenerative changes (Figure 4, DN) were observed in pristane (4c), all B19 NS1 ApoBods treated groups (4d-f) and staurosporine ApoBods groups (4g-i). Neuronal degeneration is characterized by shrinking cell bodies with eosinophilic (pink) stained cytoplasm and pyknotic nucleus (Garman, 2011). Pyknosis in neurons was observed especially in pristane group (Figure 4c, “Py”). Pyknosis is a phase of cellular necrosis, and it is due to chromatin condensation (Datta, 2004). In Figure 4c, pyknotic neurons are indicated by the letters “Py” in the lower right of the panel. The whole cell is stained purple and the nucleus is dark and condensed. In addition, empty spaces in the neuropil (Figure 4, Np) surrounding the neuron bodies suspected as demyelination (Figure 4, black arrows) were found in the brain of 50 µg (4e), and 100 µg (4f) B19 NS1 ApoBods treated mice, and in 100 µg staurosporine mice (4i).

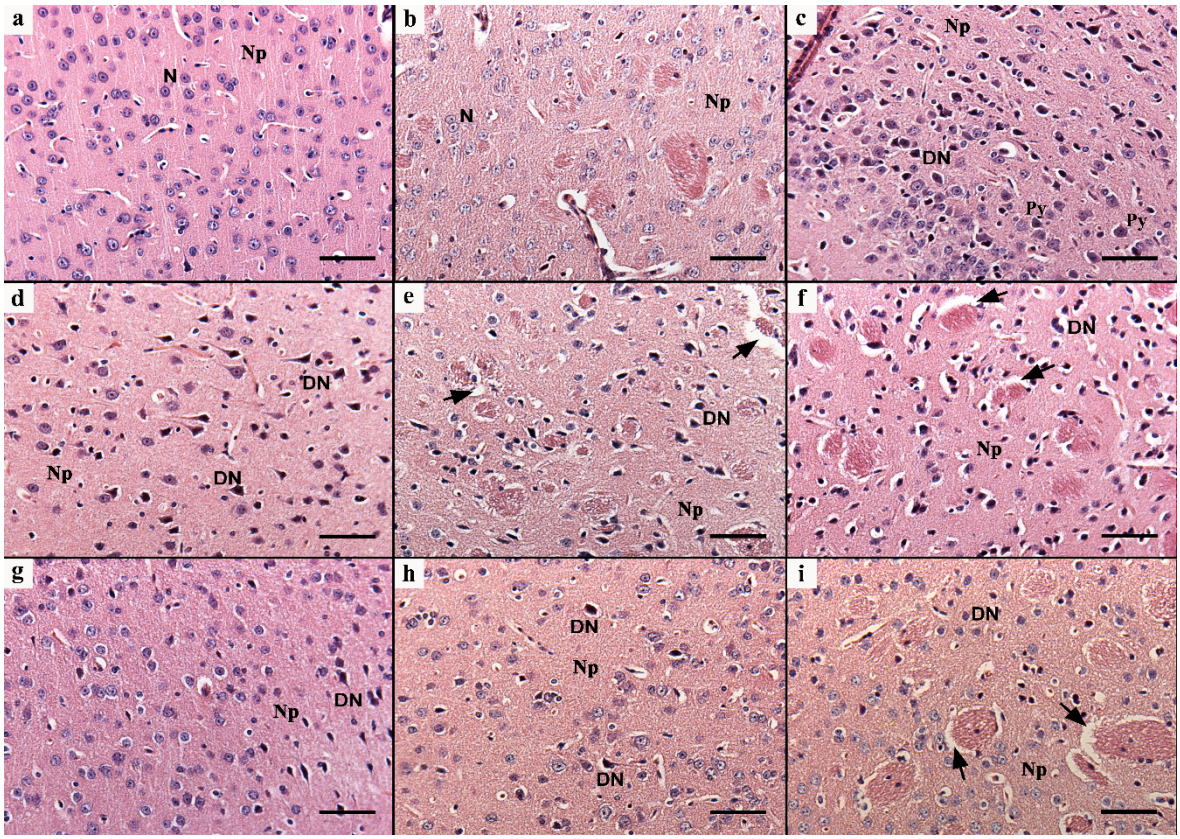

Figure 4. Histological examination of mice brain. 5 µm sections cut from paraffin blocks were stained with H&E. Representative bright-field images acquired with a 20x objective of each treatment group are presented. A) untreated, b) PBS, c) pristane, d) 25 µg, e) 50 µg, and f) 100 µg B19 NS1 ApoBods, g) 25 µg, h) 50 µg, and i) 100 µg staurosporine ApoBods. Panels a and b illustrate normal brain histology. Cellular organization is normal and there are no degenerative or demyelinating changes. Np = neuropil, N = neuron, Py = pyknosis. Degeneration of neurons (DN) was observed in pristane (c) and all B19 NS1 ApoBods (d-f), and staurosporine ApoBods treated groups (g-i). Suspected demyelination (black arrows) was found in 50 µg and 100 µg B19 NS1 ApoBods (e and f), and also in 100 µg staurosporine ApoBods (i) groups. Original magnification 20x, scale bar 200 µm.

Figures 5a and 5b illustrate normal histology of mouse kidneys. Immune cell infiltrates were not found anywhere in the kidneys of these mice. However, immune cell infiltrations pointed out by the black arrows in Figure 5, were observed in pristane group (5c), and in all B19 NS1 ApoBods treated groups (5d-f) as well as in all staurosporine ApoBods groups (5g-i). Aggregations of more than ten immune cells (cells stained dark blue) in the tissues were accounted as immune cell infiltrates. In kidneys (Figure 5), these infiltrates were mostly located in the proximity of the glomeruli but were also found more distantly. Glomeruli appeared rather normal in every group. They were round and not enlarged. However, the Bowman's space surrounding them was slightly enlarged in the highest dose of B19 NS1 ApoBods (5f).

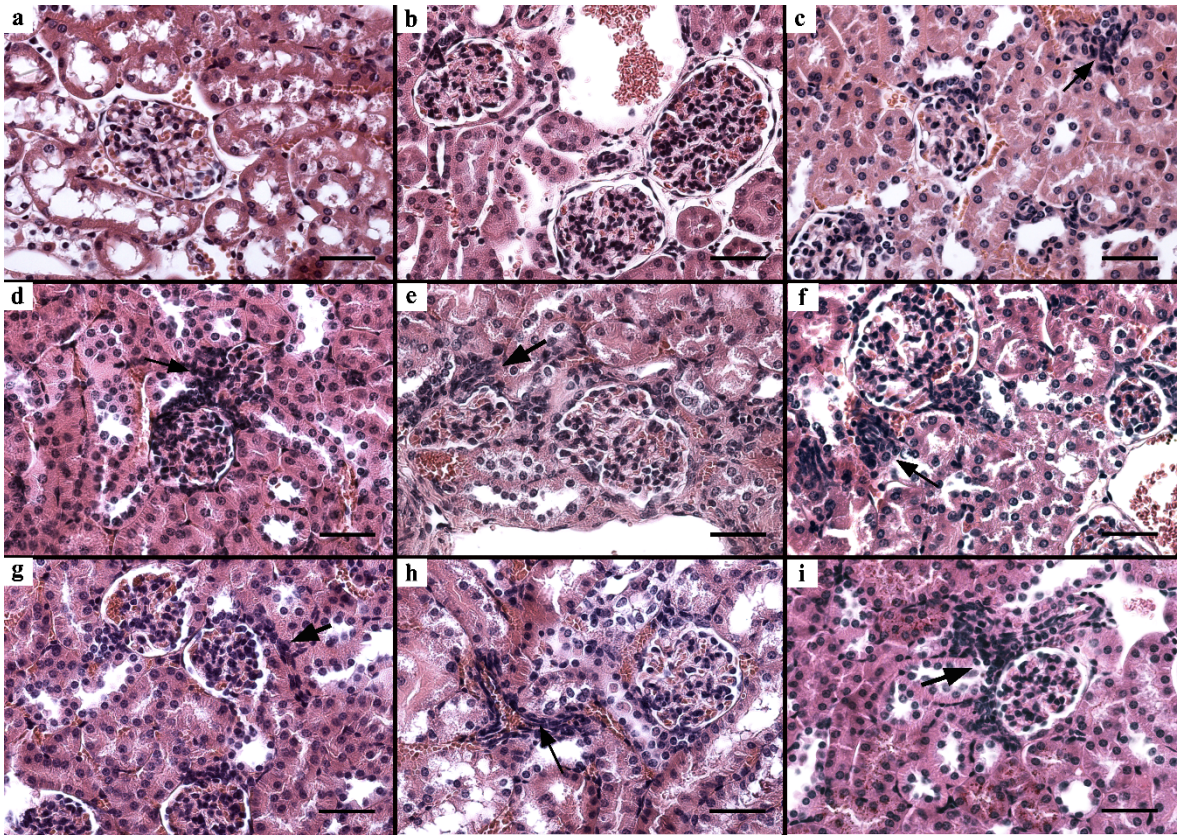

Figure 5. Histological examination of mice kidneys. 5 µm sections cut from paraffin blocks were stained with H&E. Representative bright-field images of each treatment group are presented. A) untreated, b) PBS, c) pristane, d) 25 µg, e) 50 µg, and f) 100 µg B19 NS1 ApoBods, g) 25 µg, h) 50 µg, and i) 100 µg staurosporine ApoBods. Panels a and b illustrate normal kidney histology with normal appearing glomeruli. They were regular and round. Black arrows indicate immune cell infiltrates which were observed in pristane (c), all B19 NS1 ApoBods groups (d-f) and every group of staurosporine ApoBods (g-i). Glomeruli appeared rather normal, in 100 µg B19 NS1 ApoBods (f) Bowman's space surrounding the glomeruli was slightly enlarged. Original magnification 40x. Scale bar 200 µm.

Figure 6 illustrates the representative histopathology of hearts from every treatment group. Untreated (6a) and PBS-treated (6b) present normal myocardial architecture with normal appearing cardiomyocytes. Myocytes were well organized and not swollen. Additionally, nuclei were normal sized, and there were no infiltrates in the tissues from these groups. However, infiltrates of inflammatory cells, indicated by black arrows in Figure 6, were observed in pristane (6c), all B19 NS1 ApoBods treated mice (6d-f) and in the highest dose of staurosporine ApoBods (6i). Furthermore, degenerative changes (blue arrows in Figure 6) were present in all B19 NS1 ApoBods (6d-f) and the highest staurosporine treated groups (6i). Degeneration is seen as white spaces in the cardiomyocytes as a discontinuous tissue. In contrast, vacuolation of cardiomyocytes was found only in pristane group (6c). Vacuolation is marked with VA in Figure 6c and seen as clear, round areas in the cardiomyocyte cytoplasm. Enlargement of cardiomyocyte nuclei (EN) was prominent in

highest dose of the B19 NS1 as well as staurosporine ApoBods (6f and i). Enlarged nuclei are pointed out with EN in Figure 6i and are seen on the left side of Figure 6f. Also, myocardial disarray was noted in 50 µg and 100 µg of both ApoBods (6e, f, h and i). The arrangement of myocytes is disorganized which is clearly seen on the left in 6h and the middle in 6f and 6i.

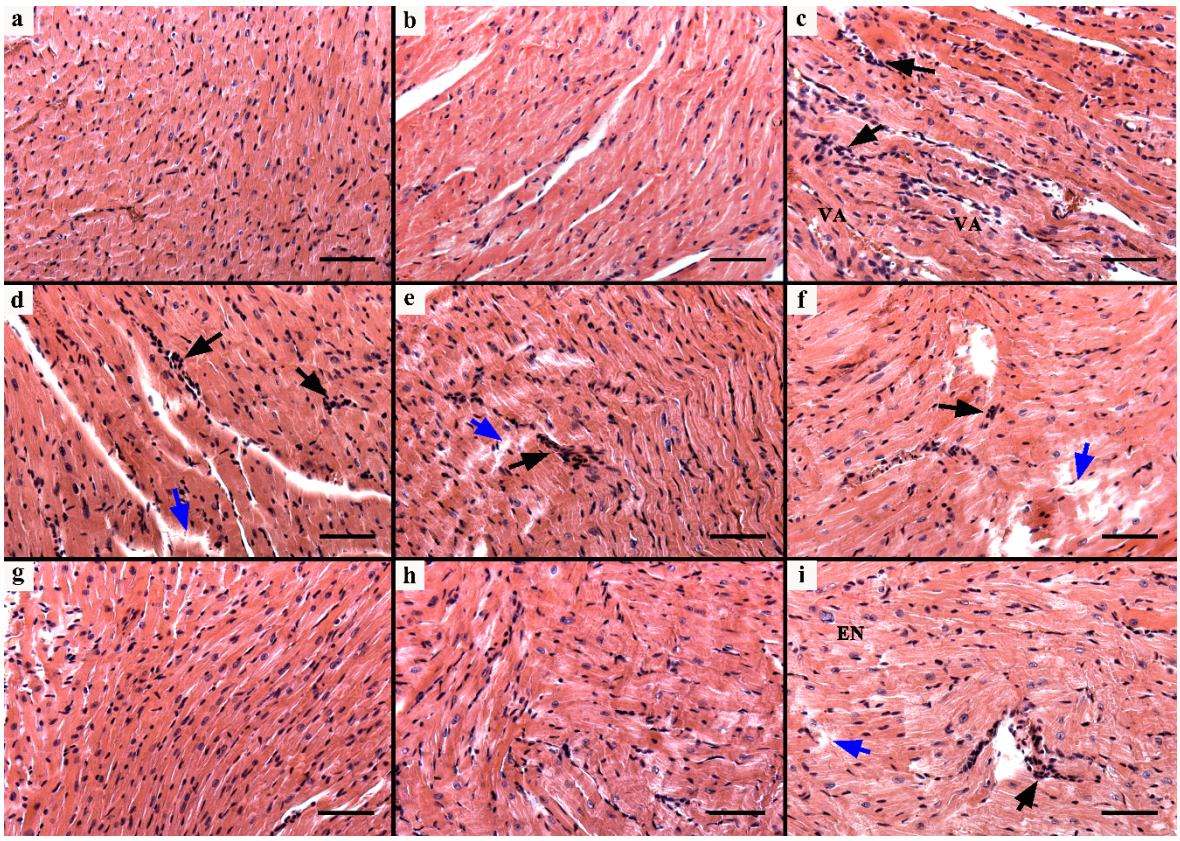

Figure 6. Histological examination of mice hearts. 5 µm sections cut from paraffin blocks were stained with H&E. Representative bright-field images acquired with a 20x objective of each treatment group are presented. A) untreated, b) PBS, c) pristane, d) 25 µg, e) 50 µg, and f) 100 µg B19 NS1 ApoBods, g) 25 µg, h) 50 µg, and i) 100 µg staurosporine ApoBods. Panels a and b illustrate normal heart histology with normal, well-organized cardiomyocytes. Infiltrations of inflammatory cells (black arrows) were observed in pristane (c), all B19 NS1 ApoBods treatment groups (d-f) and highest staurosporine dosed (i) group. In addition, myocardial degeneration (blue arrows) was present in those groups except pristane. Myocardial disarray was evident at the two highest doses of both ApoBods (e, f, h, and i). Vacuolation of cardiomyocytes (VA) was found only in pristane group (c), enlarged nuclei (EN) were prominent in highest doses of both ApoBods (f and i). Original magnification 20x, scale bar 200 µm.

The livers of untreated (Figure 7a) and PBS-treated (7b) mice demonstrated normal liver histology. There were no enlarged nuclei and only one nucleus in most of the hepatocytes. Furthermore, immune cell infiltrates were not observed in the livers of these mice. However, mononuclear cell infiltrations (black arrows in Figure 7) were observed in the livers of all the other mice: B19 NS1 ApoBods treated (7d-f) as well as in pristane (7c) and

staurosporine ApoBods groups (7g-i). In addition, karyocytomegaly meaning a single polyploid enlarged nucleus or usually two nuclei in one hepatocyte, was observed in pristane and all, B19 NS1 as well as staurosporine ApoBods treated mice. It was most prominent in the highest doses of ApoBods (7f and 7i). Enlarged nucleus and hepatocytes with two nuclei are evident in the upper left part of Figure 7i and on the right side of 7f. Furthermore, cytoplasmic vacuolation seen as round white spheres in the hepatocytes was observed in the livers of pristane-treated mice (7c, middle). Signs of extramedullary hematopoiesis were observed as well in pristane group. It was seen as a dense sack-like aggregation of cells stained dark blue at the side of a blood vessel (data not shown).

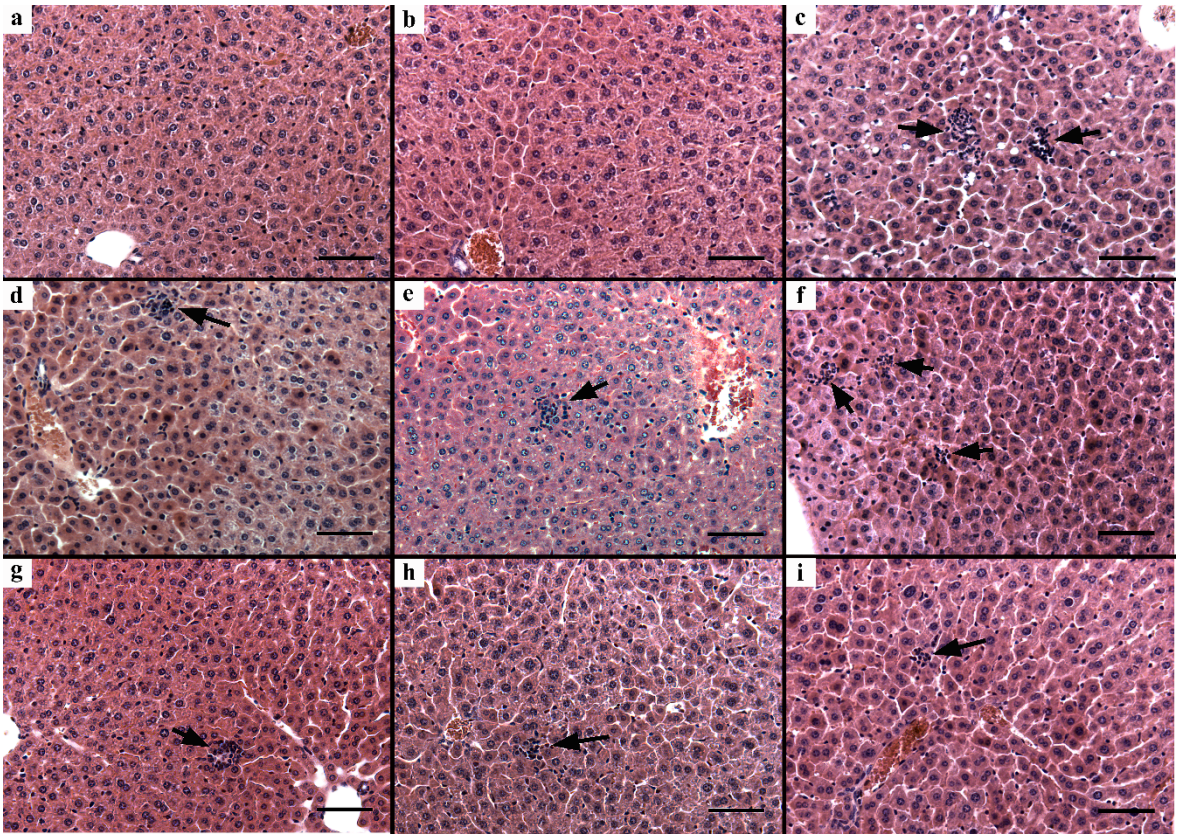

Figure 7. Histological examination of mice livers. 5 µm sections cut from paraffin blocks were stained with H&E. Representative bright-field images acquired with a 20x objective of each treatment group are presented. A) untreated, b) PBS, c) pristane, d) 25 µg, e) 50 µg, and f) 100 µg B19 NS1 ApoBods, g) 25 µg, h) 50 µg, and i) 100 µg staurosporine ApoBods. Panels a and b illustrate normal liver histology. Nuclei were normal sized; no infiltrates were observed, and most of the hepatocytes had only one nucleus. Immune cell infiltrations (black arrows) as well as karyocytomegaly (single enlarged nucleus or many nuclei in one hepatocyte) were observed in all ApoBods and pristane treatment groups. Karyocytomegaly was most prominent in highest doses of both ApoBods (f and i). In addition, cytoplasmic vacuolation (regular white spots) was noted in pristane treatment group (c). Original magnification 20x, scale bar 200 µm.

Morphological differences were observed in spleens of the mice. Spleens of untreated and PBS-treated mice illustrated normal spleen histology (Figure 8a and b, respectively). White pulp (WP) areas of the spleens in mice treated with B19 NS1 ApoBods (Figure 8d-f) as well as staurosporine ApoBods (Figure 8g-i) were more extensive than in untreated (8a), and PBS-treated (8b) mice. In higher doses the white pulp area was even greater than in lower doses. Enlargement of the white pulp follicles was more prominent in higher doses as well. Most prevalent pathologic feature in spleens of pristane treated mice (8c) was lipid accumulation (white spherical vacuoles) observed about in the tissue. Germinal centers (white arrows) had formed in the spleens of mice treated with 50 µg B19 NS1 and staurosporine ApoBods (8e and 8h, respectively).

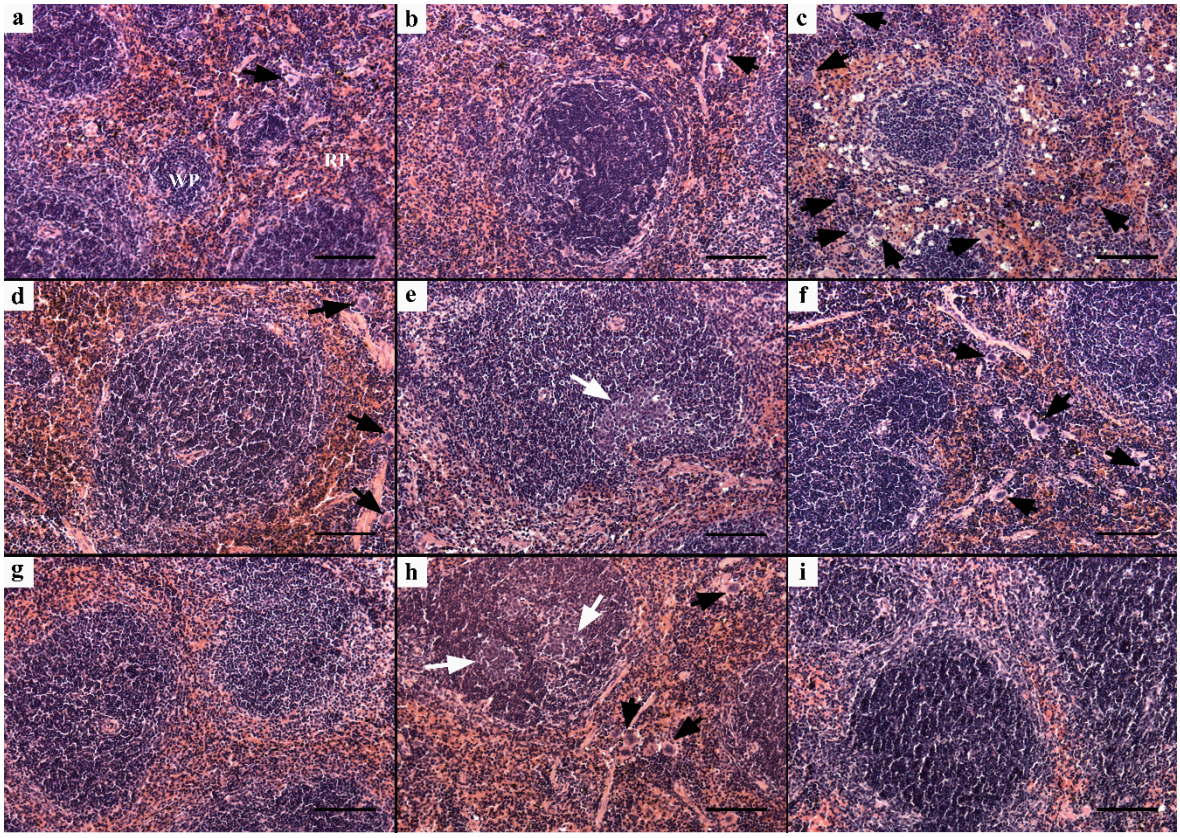

Figure 8. Histological examination of mice spleen. 5 µm sections cut from paraffin blocks were stained with H&E. Representative bright-field images of each treatment group are presented. A) untreated, b) PBS, c) pristane, d) 25 µg, e) 50 µg, and f) 100 µg B19 NS1 ApoBods, g) 25 µg, h) 50 µg, and i) 100 µg staurosporine ApoBods. Panels a and b illustrate normal spleen histology with normal appearing red (RP) and white pulp (WP) compositions. Black arrows indicate megakaryocytes that were observed in all treatment groups, most abundantly in pristane (c, 727 megakaryocytes in average, counted from one section). Lipid accumulation (white round vacuoles in c), was evident in the pristane-treated group (c). In ApoBods treatment groups (d-f and g-i), abundancy of white pulp and enlargement of follicles were more prominent and increased with the dosage. Germinal centers (white arrows) were most prominent in 50 µg of ApoBods (e and h). Original magnification 20x. Scale bar 200 µm.

5 DISCUSSION

5.1 B19 NS1 ApoBods induced autoantibody production

Anti-dsDNA antibodies are a signature biomarker of SLE (Smith and Shmerling, 1999). Their presence and concentration seem to correlate particularly with the disease flares (for review see Isenberg et al., 2007). Accordingly, it is also worthwhile to consider that anti-dsDNA antibodies can be detected even before SLE itself has developed. Furthermore, the isotope of the antibody (IgG, IgM or IgA) also plays a role because only IgG is pathogenic.

In SLE autoantibodies are produced not only against dsDNA but other nuclear, cytoplasmic, and surface molecules as well as soluble molecules, such as coagulation factors and IgG (Mok and Lau, 2003). However, this study concentrated only on anti-dsDNA antibody because it is the most important serological factor in SLE diagnosis and also in strong association with glomerulonephritis. Furthermore, anti-dsDNA antibodies aggregate into the glomeruli indicating their involvement in inflammation and pathogenesis of nephritis.

To detect anti-dsDNA antibodies from mouse serum, an ELISA protocol was developed in this study. Based on the results (Figure 3), it has proven to be functional. Moreover, in total there were three biological replicates in each group and every serum was tested in triplicates. Furthermore, three standard deviations were used in the evaluation of the results, thus giving reliability compared to the CLIFT test. Thus, the study resulted in successful development of a detection method for anti-dsDNA antibodies in mice.

CLIFT test results (Figures 1 and 2, and Table 1) deviate from those acquired with ELISA (Figure 3). A great number of cells were positive with the negative sera from untreated and PBS mice (Figure 1a and 1b, Table 1). BALB/c mice are inbred laboratory mice, thus assuring that they are pathogen-free. Binding of anti-dsDNA antibodies in this study seems unspecific with *Crithidia luciliae* cells. Low sensitivity of the CLIFT test has been reported previously (Antico et al., 2010). They compared four enzyme immunoassays for detecting anti-dsDNA antibodies in patients suffering from SLE, other connective tissue diseases, hepatitis C virus infection, or acute viral infection. CLIFT failed to detect 28 % of positive SLE patients, thus giving false negatives. In our mouse study, however, CLIFT test returned false positives. In the study by Antico et al. (2010), CLIFT test from the same

company (Euroimmun) was used, although the secondary antibody and the sera tested were human-derived. However, several studies have successfully used CLIFT for testing anti-dsDNA antibodies in mice (Gilkeson et al., 1995; Lartigue et al., 2006; Hadaschik et al., 2015). On the contrary, in this study the secondary anti-mouse antibody used was of novel design and not used with the CLIFT test before. The antibody is not even available on the market yet. Seems that in the light of the other studies, the problem here was the secondary antibody. Thus, from these two anti-dsDNA antibody detection methods, ELISA appears to be more reliable.

5.2 B19 NS1 ApoBods initiated autoimmunity and SLE-like disease in mice

B19 is known to contribute to various disorders of autoimmune nature (Lunardi et al., 2008). Furthermore, NS1 is known for its cytotoxicity (Raab et al., 2002) and cluster formation with apoptotic bodies (Thammasri et al., 2013). In non-permissive (e.g. non-erythroid) cells, overexpression of B19 NS1 initiates apoptosis by damaging DNA (Poole et al., 2011). In this study, mice were immunized with B19 NS1 ApoBods to investigate the reaction induced by these particles. As hypothesized, B19 NS1 ApoBods did induce an autoimmune reaction in mice. All the five organs, brain (Figure 4), kidneys (Figure 5), heart (Figure 6), liver (Figure 7), and spleen (Figure 8) were affected by B19 NS1 ApoBods. Thorough quantitation of the damage and degree of inflammation would take a great deal of time and would require categorizing the changes observed, for example, in grades of severity. However, by visual inspection, it seemed that overall B19 NS1 ApoBods were more deleterious than those induced by staurosporine. It could be seen especially in the heart (Figure 6). There were no infiltrates in the two lower doses of staurosporine ApoBods (Figure 6g and 6h), but in respective doses of B19 NS1 ApoBods (Figure 6d and 6e), they were evident. Pathology observed in the tissues of mice treated with B19 NS1 ApoBods (panels d-f in Figures 4-8) shared much of the same characteristics than the pristane-treated mice (panel c in Figures 4-8). Immune cell infiltrates were detected in the heart (Figure 6), liver (Figure 7), and kidneys (Figure 5) of those respective groups. Furthermore, anti-dsDNA antibodies were detected with ELISA

method (Figure 3) in B19 NS1 ApoBods mice as well as in pristane mice but not in mice treated with staurosporine ApoBods. Thus, the hypotheses are supported by these results.

Observations on the histopathology of all the organs were made based on previous literature. Degeneration of neurons in the brain was detected as described by Garman (2011): shrinking neuron cells with eosinophilic cytoplasm were observed in the brain of mice treated with B19 NS1 ApoBods (Figure 4d-f), staurosporine ApoBods (Figure 4g-i), and pristane (Figure 4c). Furthermore, the nucleus was usually pyknotic meaning darkly stained and shrunken (Garman, 2011). As shown by the pristane and ApoBods mice brain Figures 4c-i, heterogeneous environment with different stages of degeneration was indeed detected. These findings in the brain resemble the most of those made by Sibbitt et al. (2009). They studied 200 patients with neuropsychiatric SLE, and contrasted findings by magnetic resonance imaging with the histopathological findings made after 22 of the patients had died. Diffuse neuronal loss and eosinophilic degeneration were observed in some of the patients' brains. These findings were characterized as events of seizure disorders associated with SLE. In addition, demyelinating diseases are linked to SLE (Muscal and Brey, 2010). In the central nervous system, the most common demyelinating disease is multiple sclerosis (Love, 2006). For more accurate and better detection of demyelination in the brain, samples should be stained with Luxol Fast Blue (Urich et al., 2006).

In spleen, the formation of germinal centers (GC in Figure 8e and 8h) might be due to increasing need of phagocytosing cells (Shao and Cohen, 2011). If apoptotic clearance is impaired, there is a vast source of self-antigens available also in germinal centers. Apoptotic debris from autoreactive cells is present in germinal centers due to clonal selection (Shinall et al., 2000). Furthermore, germinal centers act as the site for memory B cell generation. Interestingly, germinal centers were detected only in mice treated with 50 μg of B19 NS1 and staurosporine ApoBods (Figure 8e and 8h, respectively). The altered composition of the spleen in B19 NS1 ApoBods treated mice (Figure 8d-f) may be due to induced anemia. B19 causes anemia because it infects erythrocyte progenitors (for review see Young and Brown, 2004) which then undergo apoptosis. That might explain the observation that the area of red pulp in spleens of mice treated with B19 NS1 ApoBods was markedly reduced (Figure 8d-8f) compared to the normal spleens of untreated and PBS-treated mice (Figure 8a-b). The difference was evident when inspecting the whole

tissue section. Images were acquired covering most of the tissue sample, but to save space, only the representative images of each group are presented. Moreover, enlargement of white pulp might be explained by the normal function of the spleen. The spleen starts immune responses to blood-borne antigens, and it filters blood and harbors lymphocytes, dendritic cells, macrophages, and plasma cells (Cesta, 2006). Thus, it would be rational that the immune cell storage is enlarged during infection and immune reaction. Furthermore, germinal centers form as a response to antigenic stimulation. The reason they were not detected in the highest doses of ApoBods (Figure 8f and 8i), remains unresolved. Cesta (2006) described in his article that after antigenic stimulation spleen follicles can contain germinal centers. Furthermore, extramedullary hematopoiesis was described of giving mouse spleen a blueish coloration with H&E staining. Signs of extramedullary hematopoiesis were observed not only in the spleen but liver of pristane-treated mice (Figure 7c). It is a feature that occurs during increased demand for e.g. erythrocytes, caused by anemia or inflammation (Cesta, 2006). The liver will be discussed more thoroughly later.

Infiltrates of immune cells in the kidneys were explicitly distinguished. To detect the changes in the glomeruli, kidney samples should have been examined with higher magnification. For instance, the capillaries inside glomeruli would have been of interest, since different stages of glomerulonephritis are distinguished by the changes in the glomeruli (Le Hir, 2004). However, no signs of nephritis had developed in this study, but inflammation was marked (Figure 5c-i), nevertheless. Bender et al. (2014) described a mouse study where they compared three different pristane-induced lupus mouse models. BALB/c mice were compared with NZB/W, DBA/1, and SJL mice as a model for lupus. NZB/W mice are genetically lupus-prone, in the other strains lupus is induced with pristane. In their study, BALB/c mice developed lower titers of anti-dsDNA antibodies than the others. In addition, the development of nephritis was slower. Consequently, the kidneys were still functional, all of the BALB/c strain mice were alive after five weeks from pristane injection whereas the SJL strain mice started dying after four weeks. Additionally, BALB/c mice developed arthritis. In our study, the mice were observed daily during the whole experiment of eight weeks in case of arthritis-like symptoms. However, no signs of arthritis were observed. Although there are differences between mouse strains and disease manifestations, so is between the subsets in human patients. Nevertheless,

mouse models of lupus are still comparable with the human lupus manifestations. If given more time, the B19 NS1 ApoBods treated mice might have developed nephritis since in the study of Bender et al. (2014), BALB/c mice developed some signs of nephritis during their lifespan (5 months), although slower and of lesser severity than the other strains. Also, arthritis might have emerged.

Thoolen et al. (2010) have described lesions of mouse hepatobiliary system. Accordingly, cytoplasmic vacuolation of hepatocytes was seen in livers of the pristane-treated mice (Figure 7c). It is sufficient to describe the change only as cytoplasmic vacuolation of hepatocytes, although the feature can be classified in macrovesicular and microvesicular fatty change. However, the vacuolation observed in this study resembles closely what Hardisty and Brix (2005) have described as nonzonal macrovesicular lipid accumulation. Karyocytomegaly meaning polyploid and multinucleated hepatocytes were observed most prominently in the livers of mice treated with 100 µg of either ApoBods (Figure 7f and 7i). Thoolen et al. (2010) described karyocytomegaly as a normal finding especially in aging mice, although it can be induced by, for example, drugs. Hence, formation and processing of ApoBods, especially those with viral proteins, are inducing multiplication of nuclear material without cytokinesis.

Mononuclear cell infiltration was observed in the livers of all B19 NS1 ApoBods treated groups (Figure 7d-f) as well as in the staurosporine ApoBods groups (Figure 7g-i), and in the pristane-treated group (7c). Thoolen et al. (2010) have classified infiltration to neutrophil and mononuclear, amongst other things. In this case, such a specification was not necessary since the focus was mainly to demonstrate that there are infiltrations in the tissues. However, the infiltration observed is seemingly due to B19 NS1 as was observed by Tsai et al. (2013). In their studies, only those mice that were inoculated with B19 NS1 developed hepatic infiltrates and not those that received B19 viral protein 1 or 2. This further strengthens the idea that NS1 is a crucial contributor to SLE pathogenesis.

Immune cell infiltrates were observed in the hearts of all mice treated with B19 NS1 ApoBods (Figure 6d-f), the highest dose of staurosporine ApoBods (Figure 6i), and pristane mice (Figure 6c). Additionally, degeneration of cardiomyocytes (blue arrows in Figure 6) was observed in all those groups except pristane. The presence of lymphocytic infiltrates in the hearts of mice is an indication of myocarditis that is an inflammation of

the heart (for review see Feldman, 2000). Myofibrillar disarray was observed in the hearts of mice treated with the two highest doses of B19 NS1 (Figure 6e-f) and staurosporine ApoBods (Figure 6h-i). It is a pathologic feature characterized by an abnormal alignment and joining of cardiomyocytes (Fineschi et al., 2005). In McConnell and others' (1999) study, myofibrillar disarray was associated with dilated cardiomyopathy, a heart disease with thickening of cardiac walls and enlargement of chambers. This disease is a possible consequence of viral myocarditis (for review see Feldman, 2000). Furthermore, enlargement of cardiomyocyte nuclei was observed in the highest doses of both ApoBods (EN in Figure 6f and i). The enlargement of cardiomyocyte nuclei might be due to regenerative changes responding to ApoBods. In adult mice, cardiomyocytes do not proliferate by normal cell division (for review see Senyo et al., 2014). Instead, they increase the DNA content in the nuclei, thus probably enlarging it. In pristane-treated mice, vacuolation of cardiomyocytes (VA in Figure 6c) was observed. Jokinen et al. (2011) described myocardial degeneration including vacuolation of cardiomyocytes in a cardiac toxicity study where they treated mice with diethanolamine for thirteen weeks.

6 CONCLUSIONS

B19 NS1 ApoBods are deleterious to vital tissues in BALB/c mice. They induce morphological and pathological changes in the brain, heart, kidneys, liver, and spleen. Furthermore, the contribution of the viral NS1 protein is indeed vast in the development of these changes. Hypotheses were supported by the results: inflammation was seen in the tissues and anti-dsDNA antibodies were detected in mice sera. That refers to the induction of an SLE-like disease in mice that were inoculated with B19 NS1 ApoBods. This study provides a mechanism of the association of B19 in the pathogenesis of SLE. NS1 induces apoptosis in host cells leading to the formation of ApoBods. Self-tolerance breaks when self-antigen-containing ApoBods accumulate in the tissues. The resulting cycle leads to autoimmune diseases such as SLE. Furthermore, these findings are applicable in studies of cytomegalovirus and Epstein-Barr. They both have been associated with, for example, multiple sclerosis (Love, 2006). Thus, this study gives a solid basis for more extensive studies on pathogenic viruses in the future.

7 REFERENCES

Antico, A., S. Platzgummer, D. Bassetti, N. Bizzaro, R. Tozzoli, and D. Villalta on behalf of SIMeL, Study Group on Autoimmune Diseases of the Italian Society of Laboratory Medicine. 2010. Diagnosing systemic lupus erythematosus: new-generation immunoassays for measurement of anti-dsDNA antibodies are an effective alternative to the Farr technique and the *Crithidia luciliae* immunofluorescence test. *Lupus.* 19 (8): 906-912.

Baron, S. 1996. Medical Microbiology. 4th edition. Galveston, Texas: Galveston (TX) University of Texas Medical Branch at Galveston.

Bender, A. T., Y.Wu, Q.Cao, Y.Ding, J.Oestreicher, M.Genest, S.Akare, S.T.Ishizaka, and M.F.Mackey. 2014. Assessment of the translational value of mouse lupus models using clinically relevant biomarkers. *Transl Res.* 163 (6): 515-532.

Bossuyt, X., S. Cooreman, H. De Baere, P. Verschueren, R. Westhovens, D. Blockmans , and G. Mariën . 2013. Detection of antinuclear antibodies by automated indirect immunofluorescence analysis. *Clin Chim Acta.* 415 (2013): 101-106.

Bültmann, B. D., K. Klingel, K. Sotlar, C. T. Bock, H. A. Baba, M. Sauter , and R. Kandolf. 2003. Fatal parvovirus B19-associated myocarditis clinically mimicking ischemic heart disease: An endothelial cell-mediated disease. *Hum Pathol.* 34 (1): 92-95.

Buzzulini, F., A. Rigon, P. Soda, L. Onofri, M. Infantino, L. Arcarese, G. Iannello, and A. Afeltra. 2014. The classification of *Crithidia luciliae* immunofluorescence test (CLIFT) using a novel automated system. *Arthritis Res Ther.* 16 (R71).

Cesta, M. F. 2006. Normal Structure, Function, and Histology of the Spleen. *Toxicol Pathol.* 34 (5): 455-465.

Clewley, J. P. 1984. Biochemical Characterization of a Human Parvovirus. *J Gen Virol.* 65 (1): 241-245.

Datta, B. 2004. Textbook of Pathology. 2nd edition. New Delhi, India: Jaypee Brothers Medical Publishers (P) Ltd.

Elmore, S. 2007. Apoptosis: A Review of Programmed Cell Death. *Toxicol Pathol.* 35 (4): 495-516.

Feldman, A. M. and D. McNamara. 2000. Myocarditis. *N Engl J Med.* 343 (19): 1388-1398.

Fineschi, V., M. D. Silver, S. B. Karch, M. Parolini, E. Turillazzi, C. Pomara , and G. Baroldi. 2005. Myocardial disarray: an architectural disorganization linked with adrenergic stress? *Int J Cardiol.* 99 (2): 277-282.

Garman, R. H. 2011. Histology of the Central Nervous System. *Toxicol Pathol.* 39 (1): 22-35.

Gerlach, S., K. Affeldt, L. Pototzki, C. Krause, J. Voigt, J. Fraune, and K. Fechner. 2015. Automated Evaluation of *Crithidia luciliae* Based Indirect Immunofluorescence Tests: A Novel Application of the EUROPattern-Suite Technology. *J Immunol Res.* 2015. Article ID 742402. 8 p. 2015. doi:10.1155/2015/742402.

Gilkeson, G. S. A. M. M. Pippen, and D. S. Pisetsky. 1995. Induction of Cross-Reactive Anti-dsDNA Antibodies in Preautoimmune NZB/NZW Mice by Immunization with Bacterial DNA. *J Clin Invest.* 96 1398-1402.

Gulinello, M. and C. Putterman. 2010. The MRL/lpr Mouse Strain as a Model for Neuropsychiatric Systemic Lupus Erythematosus. *J Biomed Biotechnol.* 2011. Article ID 207504. 15 p. doi:10.1155/2011/207504.

Hadaschik, E. N., X. Wei, H. Leiss, B. Heckmann, B. Niederreiter, G. Steiner, W. Ulrich, A. H. Enk, J. S. Smolen, and G. H. Stummvoll. 2015. Regulatory T cell-deficient scurfy mice develop systemic autoimmune features resembling lupus-like disease. *Arthritis Res Ther*. 17: 35. doi 10.1186/s13075-015-0538-0.

Hardisty, J. F. and A. E. Brix. 2005. Comparative Hepatic Toxicity: Prechronic/Chronic Liver Toxicity in Rodents. *Toxicol Pathol.* 33 (1): 35-40.

Hatakka, A., J. Klein, R. He, J. Piper, E. Tam, and A. Walkty. 2011. Acute Hepatitis as a Manifestation of Parvovirus B19 Infection. *J Clin Microbiol.* 49 (9): 3422-3424.

Heegaard, E. D. and K. E. Brown. 2002. Human Parvovirus B19. *Clin Microbiol Rev.* 15 (3): 485-505.

Hemauer, A., K. Beckenlehner, H. Wolf, B. Lang, and S. Modrow. 1999. Acute parvovirus B19 infection in connection with a flare of systemic lupus erythematodes in a female patient. *J Clin Virol.* 14 (1): 73-77.

Isenberg, D. A., J. J. Manson, M. R. Ehrenstein, and A. Rahman. 2007. Fifty years of anti-dsDNA antibodies: are we approaching journey's end? *Rheumatology.* 46 (7): 1052-1056.

Jokinen, M. P., W. G. Lieuallen, M. C. Boyle, C. L. Johnson, D. E. Malarkey, and A. Nyska. 2011. Morphologic Aspects of Rodent Cardiotoxicity in a Retrospective Evaluation of National Toxicology Program Studies. *Toxicol Pathol.* 39 (5): 850-860.

Jung, J. and C. Suh. 2015. Incomplete clearance of apoptotic cells in systemic lupus erythematosus: pathogenic role and potential biomarker. *Int J Rheum Dis.* 18 (3): 294-303.

Kerr, J. F. R., A. H. Wyllie, and A. R. Currie. 1972. Apoptosis: A Basic Biological Phenomenon with Wide-ranging Implications in Tissue Kinetics. *Br J Cancer.* 26 (4): 239-257.

Kivovich V, L. Gilbert, M. Vuento, and SJ. Naides. 2010. Parvovirus B19 Genotype Specific Amino Acid Substitution in NS1 Reduces the Protein's Cytotoxicity in Culture. *Int J Med Sci* 2010; 7(3):110-119. doi:10.7150/ijms.7.110.

Krygier, D. S., U. P. Steinbrecher, M. Petric, S. R. Erb, S. W. Chung, C. H. Scudamore, A. K. Buczkowski, and E. M. Yoshida. 2009. Parvovirus B19 induced hepatic failure in an adult requiring liver transplantation. *World J Gastroenterol: WJG.* 15 (32): 4067-4069.

Kühl, U., M. Pauschinger, T. Bock, K. Klingel, P. L. Schwimmbeck, B. Seeberg, L. Krautwurm, W. Poller, H. Schultheiss, and R. Kandolf. 2003. Parvovirus B19 Infection Mimicking Acute Myocardial Infarction. *Circulation.* 108 945-950.

Lartigue, A., P. Courville, I. Auquit, A. François, C. Arnoult, F. Tron, D. Gilbert, and P. Musette. 2006. Role of TLR9 in Anti-Nucleosome and Anti-DNA Antibody Production in lpr Mutation-Induced Murine Lupus. *J Immunol*. 177 (2): 1349-1354.

Le Hir, M. 2004. Histopathology of humorally mediated anti-glomerular basement membrane (GBM) glomerulonephritis in mice. *Nephrol Dial Transplant.* 19 (7): 1875-1880.

Lehmann, H. W., P. von Landenberg, and S. Modrow. 2003. Parvovirus B19 infection and autoimmune disease. *Autoimmun Rev.* 2 (4): 218-223.

Leiss, H., B. Niederreiter, T. Bandur, B. Schwarzecker, S. Blüml, G. Steiner, W. Ulrich, J. Smolen, and G. Stummvoll. 2013. Pristane-induced lupus as a model of human lupus arthritis: evolvement of autoantibodies, internal organ and joint inflammation. *Lupus.* 22 (8): 778-792.

Love, S. 2005. Demyelinating diseases. *J Clin Pathol.* 59 (11): 1151-1159.

Lunardi, C., E. Tinazzi, C. Bason, M. Dolcino, R. Corrocher, and A. Puccetti. 2008. Human parvovirus B19 infection and autoimmunity. *Autoimmun Rev; Special Issue on Infections Rheumatism and Autoimmunity.* 8 (2): 116-120.

McConnell, B. K., K. A. Jones, D. Fatkin, L. H. Arroyo, R. T. Lee, O. Aristizabal, D. H. Turnbull, D. Georgakopoulos, D. Kass, M. Bond, H. Niimura, F. J. Schoen, D. Conner, D. H. Fischman, C. E. Seidman, and J. G. Seidman. 1999. Dilated cardiomyopathy in homozygous myosin-binding protein-C mutant mice. *J Clin Invest.* 104 (9): 1235-1244.

Mok, C. C. and C. S. Lau. 2003. Pathogenesis of systemic lupus erythematosus. *J Clin Pathol.* 56 (7): 481-490.

Muscal, E. and R. L. Brey. 2010. Neurological Manifestations of Systemic Lupus Erythematosus in Children and Adults. *Neurol Clin.* 28 (1): 61-73.

Park, J., H. Lee, Y. Lee, and B. Lim. 2014. Uncleaved Dystrophin Induce Cardiac Myocyte Apoptosis in Coxsackievirus Infected Balb/C Background Mice Heart. *J Bacteriol Virol.* 44 (3): 261-268.

Perry, D., A. Sang, Y. Yin, Y. Zheng, and L. Morel. 2011. Murine Models of Systemic Lupus Erythematosus. *J Biomed Biotechnol.* 2011. Article ID 271694. 19 p. doi:10.1155/2011/271694.

Poole, B. D., V. Kivovich, L. Gilbert, and S. J. Naides. 2011. Parvovirus B19 Nonstructural Protein-Induced Damage of Cellular DNA and Resultant Apoptosis. *Int J Med Sci.* 8 (2): 88-96.

Poole, B. D., J. Zhou, A. Grote, A. Schiffenbauer, and S. J. Naides. 2006. Apoptosis of Liver-Derived Cells Induced by Parvovirus B19 Nonstructural Protein. *J Virol.* 80 (8): 4114-4121.

Raab, U., K. Beckenlehner, T. Lowin, H. Niller, S. Doyle, and S. Modrow. 2002. NS1 Protein of Parvovirus B19 Interacts Directly with DNA Sequences of the p6 Promoter and with the Cellular Transcription Factors Sp1/Sp3. *Virology.* 293 (1): 86-93.

Reeves, W. H., P. Y. Lee, J. S. Weinstein, M. Satoh, and L. Lu. 2009. Induction of autoimmunity by pristane and other naturally-occurring hydrocarbons. *Trends Immunol.* 30 (9): 455-464.

Ruehl-Fehlert, C., B. Kittel, G. Morawietz, P. Deslex, C. Keenan, C. R. Mahrt, T. Nolte, M. Robinson, B. P. Stuart, and U. Deschl. 2003. Revised guides for organ sampling and trimming in rats and mice – Part 1: A joint publication of the RITA1 and NACAD2 groups. *Exp Toxicol Pathol.* 55 (2–3): 91-106.

Saleem, T. S. M., N. Lokanath, A. Prasanthi, M. Madhavi, G. Mallika, and M. N. Vishnu. 2013. Aqueous extract of Saussurea lappa root ameliorate oxidative myocardial injury induced by isoproterenol in rats. *J Adv Pharm Technol Res.* 4 (2): 94-100.

Senyo, S. E., R. T. Lee, and B. Kühn. 2014. Cardiac regeneration based on mechanisms of cardiomyocyte proliferation and differentiation. *Stem Cell Res; Heart Regeneration and Rejuvenation.* 13 (3): 532-541.

Shao, W. and P. L. Cohen. 2011. Disturbances of apoptotic cell clearance in systemic lupus erythematosus. *Arthritis Res Ther.* 13 (1): 202-202.

Shinall, S. M., M. Gonzalez-Fernandez, R. J. Noelle, and T. J. Waldschmidt. 2000. Identification of Murine Germinal Center B Cell Subsets Defined by the Expression of Surface Isotypes and Differentiation Antigens. *J Immunol.* 164 (11): 5729-5738.

Sibbitt, W. L., W. M. Brooks, M. Kornfeld, B. L. Hart, A. D. Bankhurst, and C. A. Roldan. 2009. Magnetic Resonance Imaging And Brain Histopathology In Neuropsychiatric Systemic Lupus Erythematosus. *Semin Arthritis Rheum.* 40 (1): 32-52.

Smith, E. and R. Shmerling. 1999. The American College of Rheumatology criteria for the classification of systemic lupus erythematosus: Strengths, weaknesses, and opportunities for improvement. *Lupus.* 8. 586-595.

Söderlund-Venermo, M., K. Hokynar, J. Nieminen, H. Rautakorpi, and K. Hedman. 2002. Persistence of human parvovirus B19 in human tissues. *Pathologie Biologie.* 50 (5): 307-316.

Takahashi, Y., C. Murai, S. Shibata, Y. Munakata, T. Ishii, K. Ishii, T. Saitoh, T. Sawai, K. Sugamura, and T. Sasaki. 1998. Human parvovirus B19 as a causative agent for rheumatoid arthritis. *Proc Natl Acad Sci U S A.* 95 (14): 8227-8232.

Thammasri, K., S. Rauhamäki, L. Wang, A. Filippou, V. Kivovich, V. Marjomäki, S. J. Naides, and L. Gilbert. 2013. Human Parvovirus B19 Induced Apoptotic Bodies Contain Altered Self-Antigens that are Phagocytosed by Antigen Presenting Cells. *PLoS ONE.* 8 (6): e67179.

Thoolen, B., R. R. Maronpot, T. Harada, A. Nyska, C. Rousseaux, T. Nolte, D. E. Malarkey, W. Kaufmann, K. Küttler, U. Deschl, D. Nakae, R. Gregson, M. P. Vinlove, A. E. Brix, B. Singh, F. Belpoggi, and J. M. Ward. 2010. Proliferative and Nonproliferative Lesions of the Rat and Mouse Hepatobiliary System. *Toxicol Pathol.* 38 (7 s): 5S-81S.

Tsai, C., C. Chiu, J. Hsu, H. Hsu, B. Tzang, and T. Hsu. 2013. Human Parvovirus B19 NS1 Protein Aggravates Liver Injury in NZB/W F1 Mice. *PLoS ONE.* 8 (3): e59724.

Urich, E., I. Gutcher, M. Prinz, and B. Becher. 2006. Autoantibody-mediated demyelination depends on complement activation but not activatory Fc-receptors. *Proc Natl Acad Sci U S A.* 103 (49): 18697-18702.

Young, N. S. and K. E. Brown. 2004. Parvovirus B19. *N Engl J Med.* 350 (6): 586-597.

Yung, S. and T. M. Chan. 2008. Anti-DNA antibodies in the pathogenesis of lupus nephritis - The emerging mechanisms. *Autoimmun Rev.* 7 (4): 317-321. Baron, S. 1996. Medical Microbiology. (4th edition) Galveston, Texas: Galveston (TX) University of Texas Medical Branch at Galveston.